nobiletin or auraptene, or basal diet including 2% corn oil. Body weight and food consumption were recorded biweekly. At 20 weeks of age, animals in all groups were injected intraperitoneally 1 hour before sacrifice with 5-bromo-2′-deoxyuridine (BrdU) solution (100 mg/kg body weight). Under deep ether anesthesia, blood was collected to measure testosterone hormone levels. The urogenital complex of each rat was harvested as a whole together with the seminal vesicles, then fixed in 10% phosphate-buffered formalin. Livers, kidneys, spleens, lungs, testes and tongues were also removed, weighed and fixed. After fixation for 48 h, the ventral, dorsal, lateral, anterior prostate lobes and seminal vesicles were carefully dissected into individual lobes whenever possible, and each was weighed. The tissues were routinely processed to paraffin embedded sections and stained with hematoxylin and eosin (H&E).

Histopathology and immunohistochemistry. The prostatic lesions, including adenocarcinomas (ACs) and prostatic intraepithelial neoplasm (PINs), were histopathologically diagnosed as described previously.[25,28] Since multiple proliferative epithelial lesions develop in this model, semiquantitative analysis was performed. First, additional slides stained with Azan, which showed clear contrast between epithelium and secreted material, were made. Then, relative areas of proliferating epithelium within acini were recorded with the help of an image processor for analytical pathology (IPAP: Sumika Technos Co., Osaka, Japan). Each acinus was then graded as 1 (predominantly consists of normal epithelium), 2 (predominantly consists of PIN) and 3 (predominantly consists of adenocarcinoma) for comparison among the groups. Immunohistochemistry for BrdU and SV/40 large T antigen was performed using the monoclonal mouse anti-BrdU antibodies (Dako, Glostrup Denmark) and a mouse anti-SV40 large T antigen monoclonal (Clone: PAb 101, BD PharMingen, San Diego, CA, USA), respectively. Binding was visualized with a Vectastain Elite ABC kit (Vector Laboratory, Burlingame, CA, USA) followed by light hematoxylin counterstaining to facilitate microscopic examination.

Cell culture. LNCaP, DU145, and PC3 human prostate carcinoma cell lines were purchased from the American Type Culture Collection (ATCC, Manassas, VA, USA) and cultured as monolayers in RPMI medium 1640 (Gibco, Carlsbad, CA, USA) supplemented with 10% heat-inactivated fetal bovine serum (FBS) and 0.5% penicillin/streptomycin in a 5% CO_2 atmosphere at 37°C in a humidified incubator. Nobiletin and auraptene were dissolved in dimethyl sulfoxide (DMSO, 1% v/v final) with incubation at 37°C for 2–5 h and diluted with medium to prepare a 10 mL 1×10^{-3} M solution, then filtered through a 0.22 μm millipore filter (Millipore, Billerica, MA, USA) to avoid bacteria infection just before treatment.

Cell viability and dose responses. The effect of nobiletin or auraptene on cell viability was determined with a 2-(4-iodophenyl)-3-(4-nitrophenyl)-5-(2,4-disulfophenyl)-2H-tetrazolium salt monosodium salt (WST-1) assay.[31] LNCaP (0.4×10^4 cells/well), DU145 (0.3×10^4 cells/well) and PC3 (0.4×10^4 cells/well) cells were plated in 96-well culture plates with varying concentrations of nobiletin (0, 1×10^{-6}, 1×10^{-5}, 5×10^{-5}, 1×10^{-4} and 5×10^{-4} mol/L) or auraptene (0, 1×10^{-5}, 5×10^{-5}, 1×10^{-4}, 5×10^{-4} and 1×10^{-3} mol/L) in 200 μL of culture medium in quadruplicate. After 48 h of treatment, 20 μL WST-1 was added to each well and incubated for 90 min at 37°C, then each well was measured for absorbance at the wavelength of 430 nm. Percentage cell viability was determined relative to vehicle-treated control cells, arbitrarily assigned 100% viability.

Dose response effect of these chemicals was also investigated at narrow range of concentrations in either a T_{25} flask or 6-well plate, in which apoptosis and cell cycle analysis would be performed. LNCaP cells were preincubated in T_{25} flasks (1×10^5 cells/flask), and DU145 and PC3 cells in 6-well plates (1.8×10^4 and 3×10^4, respectively). After 24 h incubation, the medium was exchanged by a fresh medium containing test chemicals at various concentrations, as shown in Fig. 1a–c, or the vehicle. After 72 h incubation, trypan blue resistant, live cell numbers were counted under a microscope. This was performed in triplicate

Quantification of apoptotic cells. We optimized the concentrations of the chemicals so that growth inhibition rates were about 50% of the vehicle-treated control value (IC_{50}) after 3 days incubation for further study. Nobiletin and auraptene-induced apoptosis in human prostate cancer cells was determined by annexin assays with a Guava Nexin kit (Guava Technologies, Inc. Hayward CA, USA) according to the manufacturer's protocol. Briefly, prostate cancer cells were treated with chemicals as described above for 72 h, trypsinized and washed three times with 1 mL of Nexin buffer. They were then centrifuged for collection and resuspended in 50 μL of Nexin buffer. Aliquots of 5 μL of Annexin V-PE and 5 μL of 7-amino-actinomycin D (7-AAD) were added to 40 μL of cells, and the mixtures were incubated on ice for 20 min under shielding from light, then analyzed with a cell analyzer, Guava PCA (Guava Technologies, Inc.)

Cell cycle analysis. After 72 h treatment of prostate cancer cells with nobiletin or auraptene, cells were trypsinized, washed twice with ice-cold phosphate-buffered saline containing 1% FBS, resuspended in 500 μL of staining solution containing 2% RNase soluion, 2.5% propidium iodide and 0.1% Triton X-100 for each sample and the cell cycle was analyzed with Guava PCA and Multicycle AV software for Windows (Phoenix Flow Systems, San Diego, CA, US).

Statistical analysis. The statistical significance of differences among the control and chemical treatment groups was determined by Scheffe's tests. Dose-dependent cell growth inhibition with regard to chemical concentration and cell viability was assessed with Spearman's correlation coefficients (ρ). $P < 0.05$ was considered statistically significant.

Results

General observations in the animal experiment. Dietary administration of test compounds of nobiletin or auraptene did not cause any adverse effects such as on the growth of rats during the study. There was no significant differences in food intake (data not shown) or the final body weights as well as absolute and relative prostate weights among the groups (Table 1). Histologically, there were no pathological lesions in the liver, kidneys, spleen, lung and testes suggesting toxicity of nobiletin

Table 1. Final body weights, relative prostate weights and serum testosterone concentrations

Treatment	No. of rats	Body weights (g)	Relative prostate weights (%)		Serum testosterone (ng/mL)
			Whole	Ventral	
Control	9	493.71 ± 40.35	0.96 ± 0.23	0.088 ± 0.021	2.02 ± 0.68
Nobiletin	9	473.15 ± 47.17	0.88 ± 0.23	0.087 ± 0.035	1.99 ± 1.08
Auraptene	9	492.56 ± 36.97	0.83 ± 0.20	0.075 ± 0.024	2.28 ± 0.79

Values are means ± SD.

doi: 10.1111/j.1349-7006.2007.00417.x

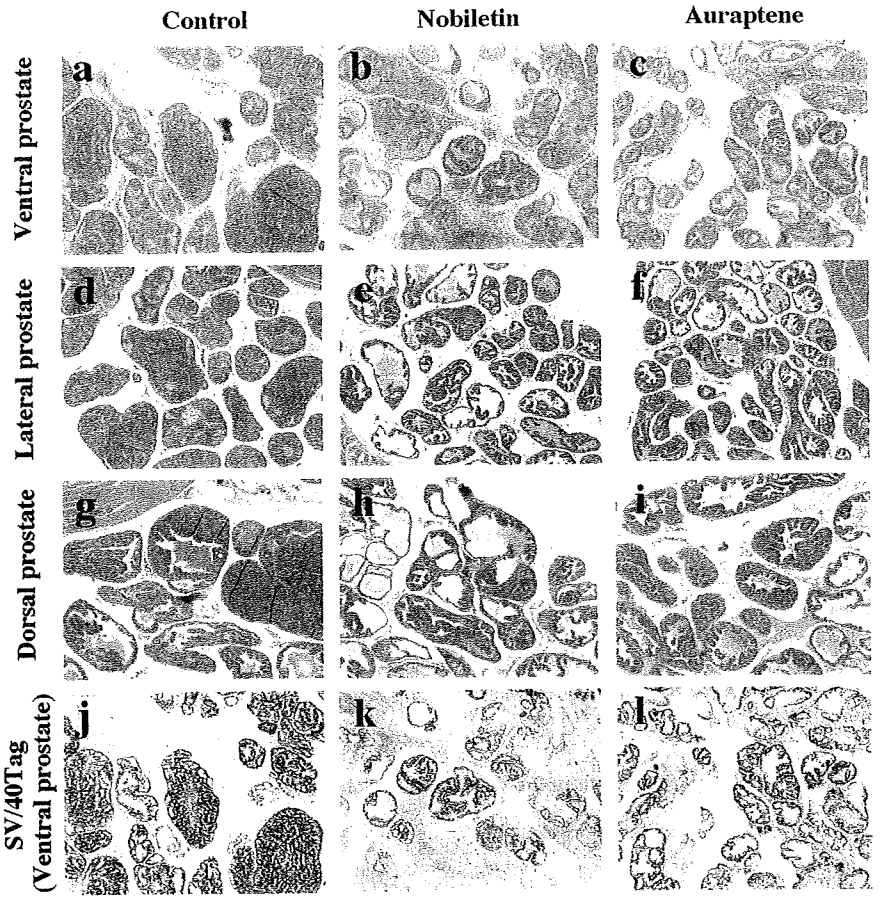

Fig. 1. Representative histological obseravation of ventral (a–c), lateral (d–f) and dorsal (g–i) prostate (hematoxylin and eosin, ×4) of transgenic rats developing adenocarcinoma of the prostate treated with vehicle control, nobiletin or auraptene. a, d, g: vehicle control group with moderatly differentiated adenocarcinoma composed of atypical epithelial cells forming glandular and cribriform structures. b, e, h: nobiletin-treated group with reduced epithelial area in ventral, lateral and dorsal prostate. c, f, i: auraptene-treated group with reduced epithelial area in lateral prostate (f). j–l: representative imunohistochemical staining of SV/40 Tag in ventral prostate. The SV/40 Tag expression in nobiletin-treated group (k) are found decreased in adenocarcinoma as compared with control group (j).

Table 2. Relative areas of epithelial components within acini

Treatment	No. of rats	Epithelium/acinus (%)				
		Ventral	Lateral	Dorsal	Anterior	Seminal vesicle
Control	9	77.63 ± 3.28	88.09 ± 3.91	64.75 ± 7.08	25.22 ± 5.41	13.58 ± 4.38
Nobiletin	9	65.58 ± 7.64**	75.34 ± 6.68***	54.11 ± 8.69*	25.91 ± 4.25	13.92 ± 3.42
Auraptene	9	70.36 ± 6.42	78.58 ± 7.13*	55.26 ± 8.76	22.99 ± 3.71	14.22 ± 4.03

*$P < 0.05$, **$P < 0.01$, ***$P < 0.001$ *vs.* untreated cotrol transgenic rats developing adenocarcinoma of the prostate, Scheffe's test. Values are means ± SD.

or auraptene. The serum testosterone levels in rats given nobiletin or auraptene did not significantly differ from the control values (Table 1). All the TRAP rats developed prostate adenocarcinomas to some degree, so that no differences were present in the incidences of PIN and prostate cancer among the three groups. However, clear differences were noted in histopathological appearances of the prostate. The ventral and lateral prostate of untreated control TRAP rats were densely occupied by adenocarcinoma clusters (Fig. 2a.d.g) with reduced acinic lumina, while those of nobiletin or auraptene-treated TRAP rats were less dense, and presence of luminal spaces was more prominent (Fig. 2b,c,e,f,h,i). Atrophic glands with degenerative alteration of tumor epithelial cells were observed with infiltration of inflammatory cells, this being particularly frequent in the ventral prostate of nobiletin-treated TRAP rats.

Quantitative analysis of carcinoma development. Data for relative areas of proliferating epithelial components in the ventral, lateral, dorsal and anterior prostate lobes are summarized in Table 2. Dietary administration of nobiletin significantly reduced the relative epithelial component of the ventral ($P < 0.01$), lateral ($P < 0.001$) and dorsal prostate ($P < 0.05$) lobes as compared with the control values. In addition, nobiletin-treated TRAP rats significantly increased grade 2 acini, predominantly containing PIN, and decreased grade 3 acini with carcinomas in the ventral and lateral prostate as compared with control TRAP rats (Table 3). Feeding with auraptene also effectively reduced the relative epithelial component in the lateral prostate ($P < 0.05$) compared with the control rats (Table 2) and raised the proportion of grade 2 acini ($P < 0.05$), and lowered grade 3 acini ($P < 0.05$) in the lateral prostate as compared with the control values (Table 3).

Immunohistochemical findings. The mean BrdU labeling indices (Table 4) of adenocarcinomas in the ventral prostate were significantly decreased by nobiletin treatment ($P < 0.05$), with a slight tendency for reduction with auraptene ($P = 0.198$) as compared with the control. Suppression of BrdU labeling indices was also observed in the lateral, dorsal and anterior prostate lobes of the nobiletin group and in the lateral prostate of the auraptene group, but without significance. In PIN, BrdU indices tend to be reduced by nobiletin or auraptene in the ventral and lateral prostate, but the differences were not significant. On

Table 3. Quantitative evaluation of prostate lesions (%)

Treatment	No. of rats	Ventral			Lateral		
		Grade 1	Grade 2	Grade 3	Grade 1	Grade 2	Grade 3
Control	9	0.00 ± 0.00	2.94 ± 1.95	97.06 ± 1.95	0.00 ± 0.00	4.93 ± 3.38	95.07 ± 3.38
Nobiletin	9	0.20 ± 0.44	8.52 ± 6.83*	91.28 ± 7.22*	0.00 ± 0.00	18.23 ± 9.35*	81.77 ± 9.35*
Auraptene	9	0.05 ± 0.14	4.57 ± 3.33	95.39 ± 3.46	0.00 ± 0.00	18.05 ± 12.48*	81.95 ± 12.48*

*$P < 0.05$ *vs.* untreated control transgenic rats developing adenocarcinoma of the prostate, Scheffe's test; values are mean ± SD; Grade 1: Predominantly consists of normal epithelium; Grade 2: Predominantly consists of PIN; Grade 3: Predominantly consists of adenocarcinoma.

Table 4. BrdU labeling indices in prostate cancers and PINs (%)

Treatment	No. of rats	Ventral	Lateral	Dorsal	Anterior
In adenocarcinoma					
Control	9	11.72 ± 3.49	13.49 ± 7.20	9.78 ± 3.68	8.41 ± 2.19
Nobiletin	9	8.03 ± 2.42*	9.32 ± 2.09	6.97 ± 1.93	6.34 ± 1.86
Auraptene	9	9.42 ± 1.60	9.67 ± 3.75	9.57 ± 3.15	8.07 ± 2.37
In PIN					
Control	9	9.60 ± 1.35	8.16 ± 1.24	5.13 ± 1.42‡	4.91 ± 1.55‡
Nobiletin	9	8.22 ± 3.06	7.79 ± 1.89	5.63 ± 1.93	5.16 ± 2.46
Auraptene	9	8.17 ± 2.51	7.79 ± 1.82	5.66 ± 0.91‡	5.54 ± 1.68†

*$P < 0.05$ *vs.* control of corresponding lobes and lesion; †$P < 0.05$, ‡$P < 0.01$ *vs.* adenocarcinoma of corresponding lobes and treatment; Scheffe's test, Values are mean ± SD; BrdU, 5-bromo-2′-deoxyuridine; PIN, prostatic intraepithelial neoplasm.

Table 5. SV40/Tag expression ratios in prostate cancers (%)

Treatment	No. of rats	Ventral	Lateral	Dorsal	Anterior
Control	9	79.02 ± 10.53	88.36 ± 3.72	67.33 ± 8.28	58.66 ± 6.87
Nobiletin	9	62.09 ± 11.06*	82.69 ± 6.14	68.09 ± 10.56	54.80 ± 7.96
Auraptene	9	68.25 ± 10.66	82.94 ± 7.50	64.74 ± 8.28	62.37 ± 6.58

*$P < 0.05$ *vs.* untreated control transgenic rats developing adenocarcinoma of the prostate, Scheffe's test. Values are mean ± SD.

the other hand, the PIN BrdU labeling indices were lower than those for adenocarcinomas in all the prostate lobes, while only the dorsal and anterior prostate lobes of control (both $P < 0.01$) and auraptene-treated animals ($P < 0.01$ and 0.05, respectively) showed significant differences.

SV40/T-antigen oncoprotein was clearly detected immunohistochemically in areas of PIN and adenocarcinomas in the ventral, lateral, dorsal and anterior prostate (Table 5, Fig. 2j–l). The incidence of the SV40/T-antigen positive cells of adenocarcinoma in ventral prostate was significantly decreased ($P < 0.05$) in the nobiletin-treated animals. In the auraptene-treated rats, values for adenocarcinomas in the ventral prostate were lower than in control TRAP rats, but the difference was not statistically significant (Table 5).

Dose-dependent growth inhibition in human prostate cancer cells. WST-1 assays performed in 96-well plates with a wide range of concentrations of nobiletin or auraptene demonstrated significant dose-dependent growth inhibition in LNCaP, DU145 and PC3 cells, except in the auraptene-case with DU145 and PC3 cells (Fig. 3a–c). Cell counting for a narrow range of concentrations in T_{25} flasks or 6-well plates also revealed both nobiletin and auraptene to cause significant dose-dependent growth inhibition in these three cell lines (Fig. 1a–c). Significantly greater growth inhibition was consistently observed with lower doses of nobiletin than with auraptene.

Annexin assays. At the optimal IC_{50} concentrations (LNCaP, nobiletin 1.3×10^{-4}, auraptene 2.8×10^{-4} mol/L; DU145, nobiletin 1×10^{-4}, auraptene 2.7×10^{-4} mol/L; PC3, nobiletin 0.65×10^{-4}, auraptene 2.7×10^{-4} mol/L), nobiletin and auraptene induced more apoptosis of LNCaP, DU145 and PC3 cells as compared with the vehicle (Fig. 4). Values were significantly increased for early, late and/or total apoptosis in all these cell lines treated with nobiletin or auraptene.

Cell cycle analysis. Based on the effects of nobiletin or auraptene on the inhibition of cell proliferation and viability, we also examined possible inhibitory effects of the chemicals on progression through the cell cycle. Compared with the vehicle (G_0/G_1, 59.6 ± 2.3%; S, 5.5 ± 0.4%; G_2/M, 24.5 ± 1.4%), treatment of LNCaP cells with nobiletin or auraptene at about IC_{50} concentration for 72 h resulted in a significantly higher ratio of cells in the G_0/G_1 phase (75.2 ± 2.2%, $P < 0.0001$; 74.0 ± 1.7%, $P < 0.0001$, respectively), with reduction in S phase (3.2 ± 0.4%, $P < 0.0001$; 3.6 ± 0.3%, $P < 0.001$, respectively) and G_2/M phase (13.3 ± 5.1%, $P < 0.01$; 16.8 ± 0.6%, $P < 0.05$, respectively) cells (Fig. 5a–c,j). Treatment of DU145 cells with nobiletin or auraptene also resulted in significantly higher levels of G_0/G_1 phase arrest (62.8 ± 3.1%, $P < 0.05$ and 66.3 ± 2.2%, $P < 0.01$, respectively), compared with the vehicle (G_0/G_1, 56.9 ± 2.1%) (Fig. 5d–f,k). With PC3 cells, nobiletin treatment resulted in a significantly higher level of G_2/M accumulation (31.9 ± 2.2%, $P < 0.05$) compared with the control (G_2/M, 26.3 ± 0.9%). Such increase was not found with the auraptene treatment (26.5 ± 1.8%, $P = 0.98$) (Fig. 5g–i,l).

Discussion

The present study provided clear evidence that the two antioxidants nobiletin and auraptene can protect against prostate cancer

doi: 10.1111/j.1349-7006.2007.00417.x

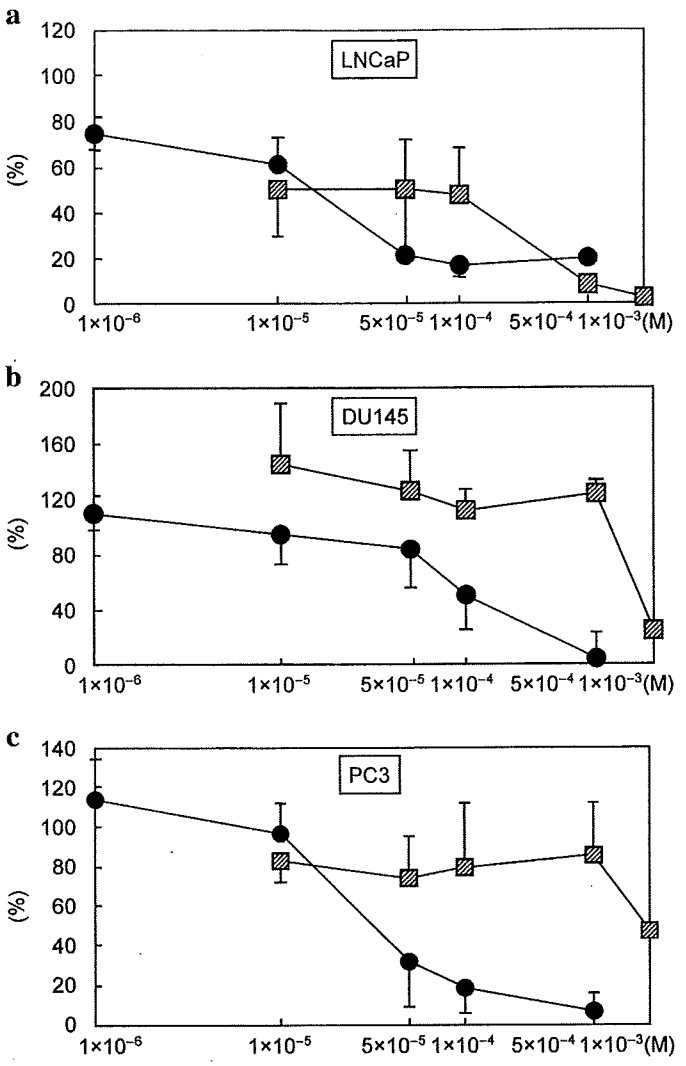

Fig. 2. Effects of nobiletin and auraptene on cell viability of prostate cancer cells (Fig. 2). The cells were exposed to a wide range of nobiletin or auraptene concentrations for 48 h, and viability of the cells was determined by WST-1 assay. Both nobiletin and auraptene caused significant dose-dependent growth inhibition in LNCaP (a) $P < 0.0001$ ($\rho = -0.87$) and $P < 0.0001$ ($\rho = -0.90$), respectively) and nobiletin also was effective in DU145 cells (b) $P = 0.0002$ ($\rho = -0.78$) and PC3 cells (c) $P < 0.0001$ ($\rho = -0.87$). Vehicle-treated cells were regarded as 100% viable, cell viabilities are depicted as percentages. The data represent the means of quadruplicate data. –●– Nobiletin, –▨– Auraptene.

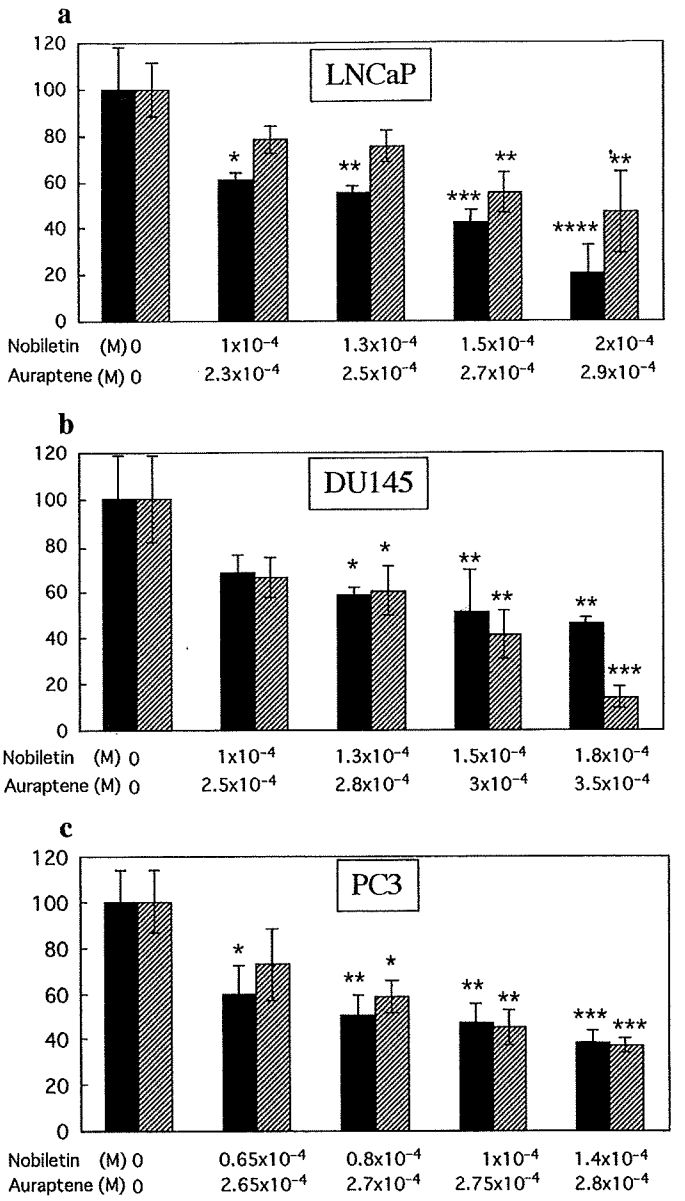

Fig. 3. Effects of nobiletin and auraptene in narrow range of concentration on cell viability of LNCaP (a), DU145 (b) and PC3 (c), evaluated with alive cell numbers after 72 h incubation. Significantly dose-dependent growth inhibition in all the three cells is seen LNCaP (a): nobiletin, $P = 0.0004$ ($\rho = -0.95$), auraptene, $P = 0.0007$ ($\rho = -0.90$); DU145 (b): nobiletin, $P = 0.001$ ($\rho = -0.87$), auraptene, $P = 0.0004$ ($\rho = -0.95$); PC3 (c): nobiletin, $P = 0.001$ ($\rho = -0.87$), auraptene, $P = 0.0006$ ($\rho = -0.92$). Columns, mean of three experiments; bars, SD. $^*P < 0.05$; $^{**}P < 0.01$; $^{***}P < 0.001$; $^{****}P < 0.0001$, *versus* control. ■ Nobiletin, ▨ Auraptene.

development in a transgenic model and also suppress proliferation by cell lines. This is in line with the earlier finding that antioxidants such as green tea polyphenols can significantly inhibit prostate cancer development and increase survival rate in transgenic adenocarcinoma mouse prostate (TRAMP) mice,[32] also bearing the SV/40 T antigen transgene under control of the probasin promoter.

Compared with chemical carcinogen induced models, including examples with 3,2′-dimethyl-4-aminobiphenyl (DMAB) and 2-amino-1-methyl-6-phenylimidazo[4,5-b]pyridine (PhIP),[33] which take 40 weeks (20 weeks after DMAB treatment for 20 weeks) and over a year, respectively, induction of prostate cancer in TRAP rats is extremely strong and rapid, even compared to the TRAMP mouse model. In TRAP rats, PIN and adenocarcinoma are found at 4 weeks and 15 weeks, respectively,[25,26] but in the TRAMP mice they are formed at 10 weeks and 18 weeks of age, respectively.[34] Cancer development in the TRAP rat largely depends on androgens, because SV40 T antigen production and cancer as well as prostate glands themselves are under the control of androgen action.[25,29] Therefore it might be expected that no effects on the incidence would be exerted without reducing the testosterone level and/or expression of SV40 T antigen in the prostate. In consequence, it is biologically significant that nobiletin or auraptene treatment here clearly suppressed tumor expansion without change in testosterone level. The fact that nobiletin and auraptene caused a shift from adenocarcinoma to PIN indicates delayed or suppressed prostate tumor progression. This might be related to inhibition of cell proliferation as revealed by reduced BrdU-labeling indices in nobiletin-treated

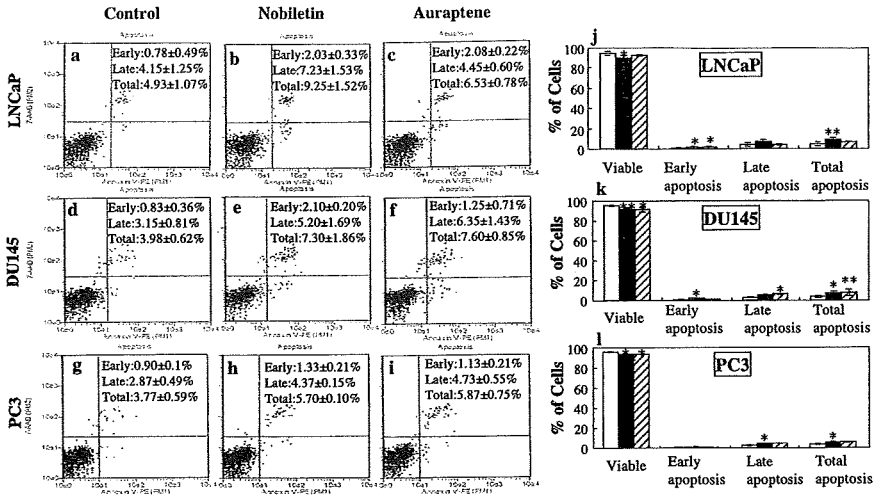

Fig. 4. Effects of nobiletin and auraptene on apoptosis induction in human prostate carcinoma cells. LNCaP cells (a–c); DU145 cells (d–f) and PC3 cells (g–i) were treated with vehicle or nobiletin or auraptene for 72 h, then harvested for analysis of apoptosis with the Guava Nexin Kit. Lower right quadrant, indicates early apoptotic cells (Annexin V-PE stained cells); upper right quadrant, indicates late apoptotic cells (Annexin V-PE and 7-AAD stained cells); lower left quadrant shows viable cells. The percentage of viable cells and early, late and total apoptosis data are summarized in j–l. Columns, mean of three experiments; bars, SD. $*P < 0.05$; $**P < 0.01$, *versus* control. □ Control, ■ Nobiletin, ▨ Auraptene.

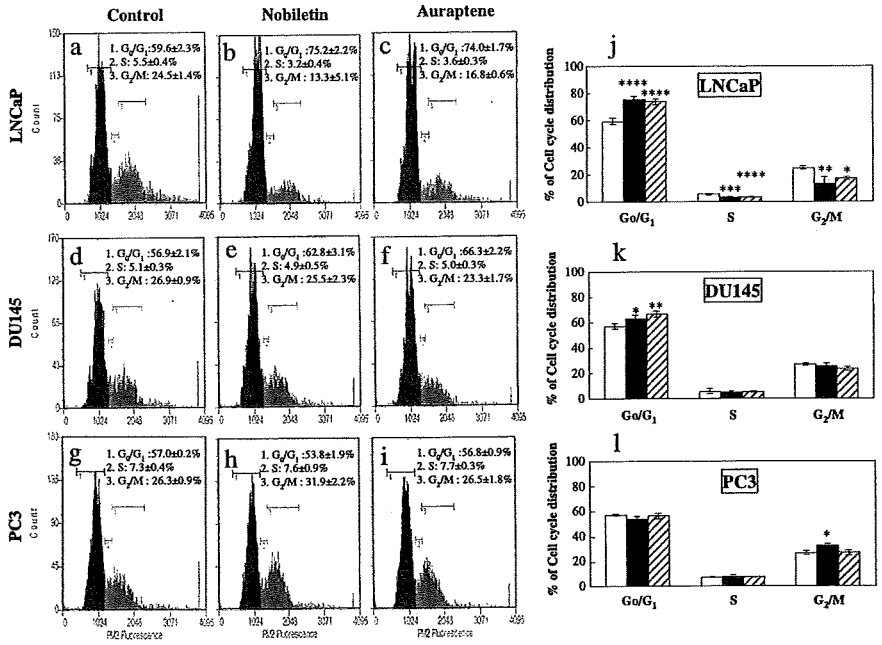

Fig. 5. Effects of nobiletin and auraptene on cell cycle progression of human prostate carcinoma cells. Cell cycle distribution in LNCaP cells (a–c) after treatment with vehicle and nobiletin or auraptene. Cell cycle distribution of DU145 and PC3 are shown in d–f and g–i, respectively. Summaries of cell cycle distribution data for LNCaP, DU145 and PC3 cells are shown in j–l. Columns, mean of three independent experiments; bars, SD. $*P < 0.05$; $**P < 0.01$; $***P < 0.001$; $****P < 0.0001$, *versus* non-treated control group. □ Control, ■ Nobiletin, ▨ Auraptene.

rats and morphometric analysis of the relative areas of epithelium in both nobiletin and auraptene-treated rats.

In our *in vitro* experiment, nobiletin or auraptene also significantly inhibited the proliferation of human prostate cancer cells, LNCaP, DU145 and PC3, in a dose-dependent fashion, and reduced their viabilities accompanied by cell cycle arrest and apoptosis induction, good markers of preventive activity.[35] It was earlier reported that the flavonoid baicalin also caused G_0/G_1 arrest in LNCaP with enhanced expression of $p27^{kip1}$[36] and in DU145[37] and the isoflavone genistein caused G_2/M arrest both in LNCaP and PC3 cells,[38,39] with down-regulation of cyclin B and up-regulation of $p21^{WAF1}$[39] and in DU145.[40] Whether the same mechanisms contribute to nobiletin and auraptene induction of G_0/G_1 arrest in LNCaP and DU145 cells, and G_2/M arrest in PC3 remains to be elucidated. Apoptosis induction is arguably the most potent defense against cancer progression,[41] and our findings for early, late or total apoptosis in LNCaP, PC3 and DU145 cells are consistent with other *in vivo* studies regarding nobiletin and auraptene[15,21] as well as *in vitro*,[36,37,42] studies of other candidates in prostate cancer cell lines.

It has been reported that lycopene, another antioxidant, exerted beneficial effects on prostate cancer prevention in an observation study and neoadjuvant intervention trial.[43] β-carotene and green tea were found to be chemopreventive for prostate cancer development in a case-control study, but had no influence in phase III and phase II studies, respectively.[43] From the present experiments, both nobiletin and auraptene should have good potential as prostate cancer preventors, but further careful investigations are required before human application.

In conclusion, the present study provided the first evidence of inhibitory effects of nobiletin and auraptene on prostate cancer in both *in vivo* and *in vitro* systems. The mechanisms appear to involve a nonandrogen-mediated pathway with induction of apoptosis and cell cycle arrest and the data suggest that nobiletin and auraptene may possess strong potential for development as chemopreventive agents against human prostate cancer.

Acknowledgments

This research was supported partly by a Grant-in-Aid for Cancer Research from the Ministry of Health, Labour and Welfare of Japan, a Grant-in-Aid for the 2nd Term Comprehensive 10-Year Strategy for Cancer Control from the Ministry of Health, Labour and Welfare of Japan, and a grant from the Society for Promotion of Pathology of Nagoya, Japan.

doi: 10.1111/j.1349-7006.2007.00417.x

References

1 Jemal A, Siegel R, Ward E *et al.* Cancer statistics, 2006. *CA Cancer J Clin* 2006; **56**: 106–30.
2 Steinmetz KA, Potter JD. Vegetables, fruit, and cancer. I. Epidemiology. *Cancer Causes Control* 1991; **2**: 325–57.
3 Li S, Yu H, Ho CT. Nobiletin: efficient and large quantity isolation from orange peel extract. *Biomed Chromatogr* 2006; **20**: 133–8.
4 Jayaprakasha GK, Negi PS, Sikder S, Rao LJ, Sakariah KK. Antibacterial activity of Citrus reticulata peel extracts. *Z Naturforsch [C]* 2000; **55**: 1030–4.
5 Murakami A, Nakamura Y, Ohto Y *et al.* Suppressive effects of citrus fruits on free radical generation and nobiletin, an anti-inflammatory polymethoxyflavonoid. *Biofactors* 2000; **12**: 187–92.
6 Murakami A, Nakamura Y, Torikai K *et al.* Inhibitory effect of citrus nobiletin on phorbol ester-induced skin inflammation, oxidative stress, and tumor promotion in mice. *Cancer Res* 2000; **60**: 5059–66.
7 Wall ME, Wani MC, Manikumar G *et al.* Plant antimutagenic agents, 2. Flavonoids. *J Nat Prod* 1988; **51**: 1084–91.
8 Nishino H, Tokuda H, Satomi Y *et al.* Cancer prevention by antioxidants. *Biofactors* 2004; **22**: 57–61.
9 Kandaswami C, Perkins E, Soloniuk DS, Drzewiecki G, Middleton E Jr. Antiproliferative effects of citrus flavonoids on a human squamous cell carcinoma in vitro. *Cancer Lett* 1991; **56**: 147–52.
10 Ohnishi H, Asamoto M, Tujimura K *et al.* Inhibition of cell proliferation by nobiletin, a dietary phytochemical, associated with apoptosis and characteristic gene expression, but lack of effect on early rat hepatocarcinogenesis in vivo. *Cancer Sci* 2004; **95**: 936–42.
11 Ishiwa J, Sato T, Mimaki Y, Sashida Y, Yano M, Ito A. A citrus flavonoid, nobiletin, suppresses production and gene expression of matrix metalloproteinase 9/gelatinase B in rabbit synovial fibroblasts. *J Rheumatol* 2000; **27**: 20–5.
12 Sato T, Koike L, Miyata Y *et al.* Inhibition of activator protein-1 binding activity and phosphatidylinositol 3-kinase pathway by nobiletin, a polymethoxy flavonoid, results in augmentation of tissue inhibitor of metalloproteinases-1 production and suppression of production of matrix metalloproteinases-1 and -9 in human fibrosarcoma HT-1080 cells. *Cancer Res* 2002; **62**: 1025–9.
13 Kawabata K, Murakami A, Ohigashi H. Nobiletin, a citrus flavonoid, down-regulates matrix metalloproteinase-7 (matrilysin) expression in HT-29 human colorectal cancer cells. *Biosci Biotechnol Biochem* 2005; **69**: 307–14.
14 Minagawa A, Otani Y, Kubota T *et al.* The citrus flavonoid, nobiletin, inhibits peritoneal dissemination of human gastric carcinoma in SCID mice. *Jpn J Cancer Res* 2001; **92**: 1322–8.
15 Suzuki R, Kohno H, Murakami A *et al.* Citrus nobiletin inhibits azoxymethane-induced large bowel carcinogenesis in rats. *Biofactors* 2004; **22**: 111–4.
16 Murakami A, Kuki W, Takahashi Y *et al.* Auraptene, a citrus coumarin, inhibits 12-O-tetradecanoylphorbol-13-acetate-induced tumor promotion in ICR mouse skin, possibly through suppression of superoxide generation in leukocytes. *Jpn J Cancer Res* 1997; **88**: 443–52.
17 Ogawa K, Kawasaki A, Yoshida T *et al.* Evaluation of auraptene content in citrus fruits and their products. *J Agric Food Chem* 2000; **48**: 1763–9.
18 Tanaka T, Kawabata K, Kakumoto M *et al.* Citrus auraptene exerts dose-dependent chemopreventive activity in rat large bowel tumorigenesis: the inhibition correlates with suppression of cell proliferation and lipid peroxidation and with induction of phase II drug-metabolizing enzymes. *Cancer Res* 1998; **58**: 2550–6.
19 Tanaka T, Kawabata K, Kakumoto M *et al.* Chemoprevention of 4-nitroquinoline 1-oxide-induced oral carcinogenesis by citrus auraptene in rats. *Carcinogenesis* 1998; **19**: 425–31.
20 Kawabata K, Tanaka T, Yamamoto T *et al.* Suppression of N-nitrosomethylbenzylamine-induced rat esophageal tumorigenesis by dietary feeding of auraptene. *J Exp Clin Cancer Res* 2000; **19**: 45–52.
21. Sakata K, Hara A, Hirose Y *et al.* Dietary supplementation of the citrus antioxidant auraptene inhibits N,N-diethylnitrosamine-induced rat hepatocarcinogenesis. *Oncology* 2004; **66**: 244–52.
22 Hara A, Sakata K, Yamada Y *et al.* Suppression of beta-catenin mutation by dietary exposure of auraptene, a citrus antioxidant, in N,N-diethylnitrosamine-induced hepatocellular carcinomas in rats. *Oncol Rep* 2005; **14**: 345–51.
23 Kohno H, Suzuki R, Curini M *et al.* Dietary administration with prenyloxycoumarins, auraptene and collinin, inhibits colitis-related colon carcinogenesis in mice. *Int J Cancer* 2006; **118**: 2936–42.
24 Tanaka T, Kohno H, Murakami M, Kagami S, El-Bayoumy K. Suppressing effects of dietary supplementation of the organoselenium 1,4-phenylenebis (methylene) selenocyanate and the Citrus antioxidant auraptene on lung metastasis of melanoma cells in mice. *Cancer Res* 2000; **60**: 3713–6.
25 Asamoto M, Hokaiwado N, Cho YM *et al.* Prostate carcinomas developing in transgenic rats with SV40 T antigen expression under probasin promoter control are strictly androgen dependent. *Cancer Res* 2001; **61**: 4693–700.
26 Cho YM, Takahashi S, Asamoto M *et al.* Age-dependent histopathological findings in the prostate of probasin/SV40 T antigen transgenic rats: lack of influence of carcinogen or testosterone treatment. *Cancer Sci* 2003; **94**: 153–7.
27 Hokaiwado N, Asamoto M, Cho YM, Tsuda H, Shirai T. Lack of effect of human c-Ha-ras proto-oncogene overexpression on prostate carcinogenesis in probasin/SV40 T antigen transgenic rats. *Cancer Sci* 2003; **94**: 1042–5.
28 Kandori H, Suzuki S, Asamoto M *et al.* Influence of atrazine administration and reduction of calorie intake on prostate carcinogenesis in probasin/SV40 T antigen transgenic rats. *Cancer Sci* 2005; **96**: 221–6.
29 Said MM, Hokaiwado N, Tang M *et al.* Inhibition of prostate carcinogenesis in probasin/SV40 T antigen transgenic rats by leuprorelin, a luteinizing hormone-releasing hormone agonist. *Cancer Sci* 2006; **97**: 459–67.
30 Asamoto M, Hokaiwado N, Cho YM, Shirai T. Effects of genetic background on prostate and taste bud carcinogenesis due to SV40 T antigen expression under probasin gene promoter control. *Carcinogenesis* 2002; **23**: 463–7.
31 Ishiyama M, Tominaga H, Shiga M *et al.* A combined assay of cell viability and in vitro cytotoxicity with a highly water-soluble tetrazolium salt, neutral red and crystal violet. *Biol Pharm Bull* 1996; **19**: 1518–20.
32 Gupta S, Hastak K, Ahmad N, Lewin JS, Mukhtar H. Inhibition of prostate carcinogenesis in TRAMP mice by oral infusion of green tea polyphenols. *Proc Natl Acad Sci USA* 2001; **98**: 10350–5.
33 Lucia MS, Bostwick DG, Bosland M *et al.* Workgroup I. rodent models of prostate cancer. *Prostate* 1998; **36**: 49–55.
34 Gingrich JR, Barrios RJ, Kattan MW, Nahm HS, Finegold MJ, Greenberg NM. Androgen-independent prostate cancer progression in the TRAMP model. *Cancer Res* 1997; **57**: 4687–91.
35 Chen C, Kong AN. Dietary cancer-chemopreventive compounds: from signaling and gene expression to pharmacological effects. *Trends Pharmacol Sci* 2005; **26**: 318–26.
36 Ikezoe T, Chen SS, Heber D, Taguchi H, Koeffler HP. Baicalin is a major component of PC-SPES which inhibits the proliferation of human cancer cells via apoptosis and cell cycle arrest. *Prostate* 2001; **49**: 285–92.
37 Gu ZQ, Sun YH, Xu CL, YL. Study of baicalin in inducing prostate cancer cell line DU145 apoptosis in vitro. *Zhongguo Zhong Yao Za Zhi* 2005; **30**: 63–6.
38 Cao F, Jin TY, Zhou YF. Inhibitory effect of isoflavones on prostate cancer cells and PTEN gene. *Biomed Environ Sci* 2006; **19**: 35–41.
39 Davis JN, Singh B, Bhuiyan M, Sarkar FH. Genistein-induced upregulation of $p21^{WAF1}$, downregulation of cyclin B, and induction of apoptosis in prostate cancer cells. *Nutr Cancer* 1998; **32**: 123–31.
40 Oki T, Sowa Y, Hirose T *et al.* Genistein induces Gadd45 gene and G2/M cell cycle arrest in the DU145 human prostate cancer cell line. *FEBS Lett* 2004; **577**: 55–9.
41 Tolomeo M, Simoni D. Drug resistance and apoptosis in cancer treatment: development of new apoptosis-inducing agents active in drug resistant malignancies. *Curr Med Chem Anticancer Agents* 2002; **2**: 387–401.
42 Chan FL, Choi HL, Chen ZY, Chan PS, Huang Y. Induction of apoptosis in prostate cancer cell lines by a flavonoid, baicalin. *Cancer Lett* 2000; **160**: 219–28.
43 Nelson PS, Montgomery B. Unconventional therapy for prostate cancer: good, bad or questionable. *Nat Rev Cancer* 2003; **3**: 845–58.

UICC
global cancer control

IJC
International Journal of Cancer

Colorectal cancer chemoprevention by 2 β-cyclodextrin inclusion compounds of auraptene and 4′-geranyloxyferulic acid

Takuji Tanaka[1,2], Mariangela B.M. de Azevedo[3], Nelson Durán[4], Joel B. Alderete[5], Francesco Epifano[6], Salvatore Genovese[6], Mayu Tanaka[7], Takahiro Tanaka[8] and Massimo Curini[9]

[1] Department of Oncologic Pathology, Kanazawa Medical University, Uchinada, Ishikawa, Japan
[2] Tohkai Cytopathology Institute: Cancer Research and Prevention (TCI-CaRP), Gifu City, Gifu, Japan
[3] Cnen/Ipen Instituto De Pesquisa Energéticas E Nucleares, Ed. Centro De Biotecnologia, Cidade Universitária, SP, Brazil
[4] Instituto de Química, Universidade Estadual de Campinas, UNICAMP, Campinas, CEP, SP, Brazil
[5] Organic Chemistry Department, Universidad de Concepción, Chile
[6] Dipartimento di Scienze del Farmaco, Università "G. D'Annunzio" di Chieti-Pescara, Chieti Scalo (CH), Italy
[7] Department of Pharmacy, Kinjo Gakuin University of Pharmacy, Moriyama-Ku, Nagoya, Aichi, Japan
[8] Department of Physical Therapy, Kansai University of Health Sciences, Kumàtori-Machi, Sennan-Gun, Osaka, Japan
[9] Dipartimento di Chimica e Tecnologia del Farmaco, Sezione di Chimica Organica, Università degli Studi di Perugia, Perugia, Italy

Carcinogenesis

The inhibitory effects of novel prodrugs, inclusion complexes of 3-(4′-geranyloxy-3′-methoxyphenyl)-2-*trans* propenoic acid (GOFA) and auraptene (AUR) with β-cyclodextrin (CD), on colon carcinogenesis were investigated using an azoxymethane (AOM)/dextran sodium sulfate (DSS) model. Male CD-1 (ICR) mice initiated with a single intraperitoneal injection of AOM (10 mg/kg body weight) were promoted by the addition of 1.5% (w/v) DSS to their drinking water for 7 days. They were then given a basal diet containing 2 dose levels (100 and 500 ppm) of GOFA/β-CD or AUR/β-CD for 15 weeks. At Week 18, the development of colonic adenocarcinoma was significantly inhibited by feeding with GOFA/β-CD at dose levels of 100 ppm (63% reduction in multiplicity, $p < 0.05$) and 500 ppm (83% reduction in the multiplicity, $p < 0.001$), when compared with the AOM/DSS group (multiplicity: 3.36 ± 3.34). In addition, feeding with 100 and 500 ppm ($p < 0.01$) of AUR/β-CD suppressed the development of colonic adenocarcinomas. The dietary administration with GOFA/β-CD and AUR/β-CD inhibited colonic inflammation and also modulated proliferation, apoptosis and the expression of several proinflammatory cytokines, such as nuclear factor-kappaB, tumor necrosis factor-α, Stat3, NF-E2-related factor 2, interleukin (IL)-6 and IL-1β, which were induced in the adenocarcinomas. Our findings indicate that GOFA/β-CD and AUR/β-CD, especially GOFA/β-CD, are therefore able to inhibit colitis-related colon carcinogenesis by modulating inflammation, proliferation and the expression of proinflammatory cytokines in mice.

There were ~1 million new cases of colorectal cancer (CRC) in 2002 (9.4% of the total cancers).[1] Globally, the mortality of CRC was reported to be 655,000 deaths per year in 2005.[2] There is at least a 25-fold variation in the occurrence of CRC worldwide.[1] The highest rates of incidence are in North America, Australia/New Zealand, Western Europe and Japan, especially in Japanese men.[1] These large geographic differences for CRC are probably explained by differences in environmental exposures and lifestyles.

There are several types of pathogenesis of CRC.[3] Among them, inflammation is linked with CRC development.[4] The risk of CRC in patients with inflammatory bowel disease

Key words: β-cyclodextrin, 4′-geranyloxyferulic acid, auraptene, inclusion compounds, antitumor activity

Abbreviations: AOM: azoxymethane; AUR: auraptene; CDs: cyclodextrins; COX: cyclooxygenase; CRC: colorectal cancer; DSS: dextran sodium sulfate; dUTP: deoxyuridine triphosphate; GOFA: 3-(4′-geranyloxy-3′-methoxyphenyl)-2-*trans* propenoic acid (4′-geranyloxy-ferulic acid); IBD: inflammatory bowel disease; IL: interleukin; iNOS: inducible nitric oxide synthase; NF-κB: nuclear factor-kappaB; Nrf2: NF-E2-related factor 2; TdT: terminal deoxynucleotidyl transferase; Tnf: tumor necrosis factor; TUNEL: TdT-mediated dUTP-biotin nick end labeling

Additional Supporting Information may be found in the online version of this article

Mayu Tanaka and Takahiro Tanaka, who contributed equally to this work, were the summer students of the Department of Oncologic Pathology at Kanazawa Medical University.

Grant sponsor: Ministry of Education, Culture, Sports, Science and Technology of Japan; Grant numbers: 18592076, 17015016; Grant sponsor: High-Technology Center of Kanazawa Medical University; Grant numbers: H2008-12, H2009-12; Grant sponsors: Ministry of Health, Labour and Welfare of Japan, Italian Ministero dell'Istruzione, Università e Ricerca (MIUR)

DOI: 10.1002/ijc.24833

History: Received 7 Apr 2009; Accepted 6 Aug 2009; Online 17 Aug 2009

Correspondence to: Takuji Tanaka, Department of Oncologic Pathology, Kanazawa Medical University, 1-1 Daigaku, Uchinada, Ishikawa 920-0293, Japan, Fax: +81-76-286-6926, E-mail: takutt@kanazawa-med.ac.jp

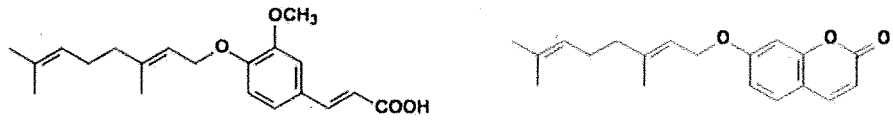

a *b*

Figure 1. Chemical structures of (*a*) 3-(4′-geranyloxy-3′-methoxyphenyl)-2-*trans* propenoic acid (GOFA) and (*b*) auraptene (AUR).

(IBD), including ulcerative colitis, increases with the increasing extent and duration of the disease.[3,5,6] A mouse model was recently established for colitis-related colon carcinogenesis[7] to facilitate the investigation of pathogenesis[8–10] and the chemoprevention[11,12] of inflammation-related CRC. In this mouse model of inflammation-related two-stage colon carcinogenesis, different types of colonic carcinogens can be used in combination with a colitis-inducing agent, such as dextran sodium sulfate (DSS), and many colonic tumors develop within a short-term period.[7,13–15] The powerful tumor-promoting effect of DSS may be due to the oxidative/nitrosative stress that is caused by DSS-induced colitis.[8–10] This suggests that the oxidative/nitrosative DNA damage associated with inflammation is involved in carcinogenesis, and, therefore, it is important to control the events that result in inflammation-related carcinogenesis.[16] In humans, the inflammatory cytokines and oxidative stress also play a key role in the pathogenesis of IBD-related intestinal damage.[17,18] As our understanding of the pathogenesis of IBD is currently inadequate, drug therapy of IBD and INB-related CRC has been empirical, *i.e.*, it is not based on a sound understanding of the etiology of the disease: drug therapy for IBD initially appears successful in the majority of IBD patients, and it comes with the risk of significant side effects. Therefore, we need new strategies, including chemoprevention, for IBD[19] and IBD-associated CRC.[3,20–23]

The natural and semisynthetic cyclodextrins (CDs) have been extensively studied to improve certain properties of the drugs, such as solubility, stability and bioavailability.[24] The CDs are suitable drug delivery systems because of their ability to greatly modify the physicochemical and biological properties of guest molecules through labile interactions by the formation of inclusion complexes. We have recently shown that modification of the physicochemical properties of violacein was achieved by the preparation of inclusion complexes with β-CD, thus leading to growth-inhibitory effects of its β-CD inclusion complexes against HL60 cells.[25–27] Many drugs currently used in the therapeutic management of colon diseases have been used as inclusion complexes with CDs.[28] The inclusion of the active principles in the cage represented by CD-protected drugs from absorption in the stomach and the upper portion of the lower intestine led to degradation of the saccharide portion in the large bowel by intestinal microflora, thereby ensuring a specific colon delivery with the maximum of bioavailability. This is the scope of the drugs that are being used in the therapy of malignant forms of colon cancer and IBD.

The 3-(4′-geranyloxy-3′-methoxyphenyl)-2-*trans* propenoic acid (4′-geranyloxy-ferulic acid, GOFA) (Fig. 1*a*) is a prenyloxycinnamic acid that was extracted from the Australian small plant *Acronychia baueri* Schott (Family, Rutaceae) in 1966, and, in the last decade, was seen to exert valuable anticancer effects, particularly against tumors affecting the gastrointestinal apparatus.[23,29] Auraptene (AUR) (Fig. 1*b*) is a geranyloxycoumarin that is widespread in the natural kingdom and was extracted from plants belonging to several families (mainly Rutaceae and Apiaceae), comprising many edible fruits and vegetables, such as lemons, grapefruits and oranges. Like GOFA, AUR was seen in recent years to exert valuable pharmacological properties,[30] including dietary feeding colon cancer chemopreventive properties.[22]

As a continuation of our studies, we aimed to acquire further insights into the anticancer properties of selected prenyloxyphenylpropanoids. In our study, we wish to report the colon cancer chemopreventive activity of 2 novel prodrugs of GOFA/β-CD and AUR/β-CD that were obtained as their inclusion complexes with β-CD, using an inflammation-associated mouse colon carcinogenesis initiated with azoxymethane (AOM) and promoted by DSS.[7] For the mechanistic investigation of the effects of the 2 prodrugs on AOM/DSS-induced tumorigenesis, we determined the immunohistochemical expression of the proinflammatory cytokines, including nuclear factor-kappaB (NF-κB),[31–33] NF-E2-related factor 2 (Nrf2),[31,34] tumor necrosis factor (Tnf)-α[35–37] and STAT3[36] in adenocarcinomas that developed in the colon. In addition, the expression of interleukin (IL)-6[38,39] and IL-1β[40] was evaluated in the colonic epithelial malignancies. The effects of GOFA/β-CD and AUR/β-CD in the diet on cell proliferation and apoptosis of colonic adenocarcinomas were evaluated using proliferating cell nuclear antigen (PCNA)[21,41] for proliferative activity, apoptosis indices by terminal deoxynucleotidyl transferase (TdT)-mediated deoxyuridine triphosphate (dUTP)-biotin nick end labeling (TUNEL) method[21] and positive rate of survivin[42] for apoptosis-inhibiting activity.

Material and Methods

Preparation of the inclusion complexes

GOFA and AUR were prepared according to previously reported methods.[43,44] β-CD was purchased from Aldrich Chemical. The inclusion complexes with a 1:1 molar ratio of

GOFA to β-CD and AUR to β-CD (113.5 mg, 0.1 mmol) were obtained by dissolving the geranyloxy derivative (0.1 mmol) in 100 mL of acetone, and soon thereafter, slowly evaporating the solution to dryness under vacuum in a rotatory evaporator at 45 C.[45] The structure of both inclusion compounds was determined by thermal analysis, X-ray diffraction, IR and NMR analysis, as already described.[46] The thermogravimetric analysis (TGA) data were obtained using a Polymer Laboratories (STA-625) thermal analyzer. The samples (2–6 mg) were heated in sealed aluminum pans under nitrogen flow (50 cm^3 min^{-1}) at a heating rate of 10 C min^{-1} from 50 to 500 C.[25,27,45,46] The powder X-ray diffraction patterns were recorded using a 6000-XRD (Shimadzu X-ray diffractometer) under the following conditions: Ni-filtered CuK radiation, voltage 40 kV, current 30 mA, at a scanning speed of 2 min^{-1} and count range 1,000 CPS. The detector was a proportional counter with a 1.7-kV detector voltage.[47–49] The samples of the solid dispersions and the physical mixtures of the complex and free drug and free CD were mixed with KBr and was pressed into a small tablet, which was mounted in the infrared beam. The spectra were recorded on the Perkin Elmer Model 1760X FTIR spectrometer from the KBr discs in the 500–4,000 cm^{-1} region.

Preclinical chemopreventive experiment

Animals, chemicals and diets. Male Crj: CD-1 (ICR) mice (Charles River Japan, Tokyo, Japan), 5 weeks of age, were used in our study. The animals were maintained in the Kanazawa Medical University Animal Facility according to the Institutional Animal Care Guidelines. All the animals were housed in plastic cages (5 mice/cage) and had free access to tap water and a pelleted Charles River Formula (CRF)-1 basal diet (Oriental Yeast, Tokyo, Japan) during quarantine under controlled conditions of humidity (50 ± 10%), lightning (12-hr light/dark cycle) and temperature [(23 ± 2) C]. They were quarantined for 7 days after arrival and randomized by body weight into the experimental and the control groups. A colonic carcinogen AOM was purchased from Sigma-Aldrich Chemical (St. Louis, MO). DSS with a molecular weight of 36,000–50,000 Da (Lot no. 6046H) was purchased from MP Biomedicals, LLC (Aurora, OH). DSS for the induction of colitis was dissolved in water at 1.5% (w/v). β-CD inclusion complexes of GOFA (GOFA/β-CD) and AUR (AUR/β-CD) were synthesized, as described earlier. The experimental diets containing 0, 100 and 500 ppm of GOFA/β-CD (MW 1465.43) or AUR/β-CD (MW 1433.39) in a powdered basal diet CRF-1 were prepared weekly in our laboratory and stored in a cold room. The doses were selected based on our previous studies.[22,23] The animals had access to food and water at all times. The food cups were replenished daily with a fresh diet. All the handling and procedures were carried out in accordance with the Institutional Animal Care Guidelines.

Experimental procedures. The Institutional Animal Care and Use Committee evaluated all the animal procedures that were associated with our study and assured that all the proposed methods were appropriate.

A total of 150 male ICR mice were divided into 5 experimental and control groups (Supporting Information Fig.). The mice in Groups 1–5 were initiated with AOM by a single intraperitoneal injection (10 mg/kg body weight). One week after the injection, 1.5% DSS (w/v) in drinking water was administrated to mice of Groups 1–5 for 7 days, followed by no further treatment for 18 weeks. The mice of Group 1 were maintained on the CRF-1 diet throughout the study. The mice of Groups 2 and 5 were fed CRF-1 diets containing 100 ppm GOFA/β-CD (Group 2), 500 ppm GOFA/β-CD (Group 3), 100 ppm AUR/β-CD (Group 4) and 500 ppm AUR/β-CD (Group 5) for 15 weeks, respectively, starting 1 week after the cessation of DSS exposure. Group 6 received AOM injection alone. Group 7 was treated with DSS alone. Groups 8 and 9 did not receive AOM and DSS and were fed CRF-1 diets containing 500 ppm GOFA/β-CD and AUR/β-CD, respectively. Group 10 did not receive any treatments and served as an untreated control. At the end of study (Week 18), all the mice were killed by CO_2 asphyxiation for careful necropsy, with emphasis on colon, liver, kidney, lung and heart.

At necropsy, the colons were flushed with saline, excised, their length measured (from ileocecal junction to the anal verge), cut open longitudinally along the main axis and then washed with saline. They were cut and fixed in 10% buffered formalin for at least 24 hr. A histological examination was performed on the paraffin-embedded sections after hematoxylin and eosin (H&E) staining by one (T.T.) of the investigators. Colonic tumors were diagnosed according to Ward's description.[50] In brief, if the tumor cells with tubular formation invaded into the depth of the submucosa, the tumor was diagnosed as adenocarcinoma. When the tumor cells with glandular structure did not invade the submucosa and compressed the surrounding crypts, the tumor was diagnosed as adenoma.

Scoring of inflammation in the large bowel. Inflammation in the large bowel was scored on the H & E-stained sections made from all the mice. For scoring, the large intestinal inflammation was graded according to the following morphological criteria[51]: Grade 0, normal appearance; Grade 1, shortening and loss of the basal 1/3 of the actual crypts with mild inflammation in the mucosa; Grade 2, loss of the basal 2/3 of the crypts with moderate inflammation in the mucosa; Grade 3, loss of the entire crypts with severe inflammation in the mucosa and submucosa, but with retention of the surface epithelium; Grade 4, presence of mucosal ulcer with severe inflammation (infiltration of neutrophils, lymphocytes and plasma cells) in the mucosa, submucosa, muscularis propria and/or subserosa. The scoring was made on the entire colon with or without proliferative lesions and expressed as a mean average score/mouse.

Immunohistochemistry of NF-κB, Nrf2, Tnf-α, Stat3, IL-6, IL-1β, PCNA, TUNEL and survivin. The immunohistochemical analysis of the colon adenocarcinomas for the antibodies of NF-κB, Nrf2, Tnf-α, Stat3, IL-6, IL-1β, PCNA, TUNEL and survivin was performed on 4-μm-thick paraffin-embedded sections by applying the labeled streptavidin biotin method

using a LSAB KIT (DAKO Japan, Kyoto, Japan), with microwave accentuation. The paraffin-embedded sections from the colonic neoplasms of the mice in each group (n = 18 in Group 1, n = 11 in Group 2, n = 6 in Group 3, n = 6 in Group 4 and n = 3 in Group 5) were heated for 30 min at 65 C, deparaffinized in xylene and rehydrated through graded ethanol at room temperature. Tris-HCl buffer (0.05 M, pH 7.6) was used to prepare the solutions and was used for the washes between the various steps. The incubations were performed in a humidified chamber.

The sections were treated for 40 min at room temperature with 2% bovine serum albumin and incubated overnight at 4 C with primary antibodies. The primary antibodies included anti-NF-κB p50 (H-119) rabbit polyclonal antibody (#sc-7178, 1:500 dilution; Santa Cruz Biotechnology, Santa Cruz, CA), anti-rabbit Nrf2 polyclonal antibody (#ab31163, 1:500 dilution; Abcam, Cambridge, MA), anti-human Tnf-α rabbit polyclonal antibody (#ab6671, 1:500 dilution; Abcam), anti-mouse Stat3 rabbit polyclonal antibody (#ab31370, 1:250 dilution; Abcam), anti-rabbit IL-6 polyclonal antibody (#ab6672, 1:400 dilution; Abcam), anti-mouse IL-1β rabbit polyclonal antibody (#LS-B40, 1:250 dilution; LifeSpan BioSciences, Seattle, WA), anti-rabbit survivin (71G4B7E) monoclonal antibody (#2808, 1:2,000 dilution; Cell Signaling Technology, Danvers, MA) and anti-human PCNA mouse monoclonal antibody (DAKO #U 7032, 1:1,000 dilution; DakoCtytomation, Kyoto, Japan). These antibodies were applied to the sections according to the manufacturer's protocol. The horseradish peroxidase activity was visualized by the treatment with H_2O_2 and 3,3′-diaminobenzidine for 5 min. At the last step, the sections were weakly counterstained with Mayer's hematoxylin (Merck, Tokyo, Japan). For each case, the negative controls were performed on the serial sections without the first antibodies.

The levels of apoptosis in tumor tissues determined by the TUNEL method were done on 4-μm formalin-fixed, paraffin-embedded tissue sections of the colonic adenocarcinomas, according to the manufacturer's instructions using the Apoptosis *in situ* Detection Kit Wako (Cat. No. 298-60201, Wako Pure Chemical Industries, Osaka, Japan). The kit is based on the TUNEL procedure. The appropriate positive and negative controls for determining the specificity of staining were generated. The negative controls were processed in the absence of the TdT enzyme in the reaction buffer. Sections of tissue digested with nuclease enzyme and colon lymphoid nodules, which are known to exhibit high rates of apoptosis, were used as the positive controls. The color was developed with the peroxidase substrate 3,3′-diaminobenzidine and the sections were counterstained with Mayer's hematoxylin (Merck).

Immunohistochemical evaluation and scoring. The immunoreactivity against the antibodies, except PCNA, TUNEL and survivin, was assessed in the large colonic adenocarcinomas (more than 3 mm in diameter) developed in Groups 1–5 using a microscope (Olympus BX41, Olympus Optical, Tokyo, Japan). The intensity and localization of the immunoreactivity against the primary antibodies were determined by a pathologist (T.T.) who was unaware of the treatment group to which the slide belonged. The immunoreactivity was evaluated against the NF-κB, Nrf2, Tnf-α, Stat3, IL-6 and IL-1β antibodies with grading between 0 and 5: 0 (−15% of the colonic cancer cells showing positive reactivity), 1 (16–30% of the colonic cancer cells showing positive reactivity), 2 (31–45% ofthe colonic cancer cells showing positive reactivity), 3 (46–60% of the colonic cancer cells presenting positive reactivity), 4 (61–75%. of the colonic cancer cells showing positive reactivity) and 5 (−75% of the colonic cancer cells showing positive reactivity).

The number of nuclei with positive reactivity for PCNA-, TUNEL- and survivin-immunohistochemistry was counted in a total of 3 100 cells in 3 different areas of the colonic cancer and expressed as a percentage (mean ± SD).

Statistical evaluation. Where applicable, the data were analyzed using 1-way ANOVA with Tukey-Kramer Multiple Comparisons Test (GraphPad Instat version 3.05, GraphPad Softwear, San Diego, CA) with $p < 0.05$ as the criterion of significance. The Fisher's exact probability test was used for comparison of the incidence of lesions between the 2 groups.

Results

General observation

During the experiment, a few animals of Groups 1–5 and 7 (DSS alone) had bloody stool, but the symptom disappeared soon after stopping the DSS treatment. At Week 18, some of the mice of Groups 1–5 had bloody stool again and anal prolapse because of rectal tumor. The mice belonging to Groups 6 (AOM alone), 8 (GOFA/β-CD alone), 9 (AUR/β-CD alone) and 10 (untreated) did not have any symptoms related to the treatments during the experimental period. As summarized in the Supporting Information Table, there was no significant change between the experimental groups with respect to the parameters tested (body and spleen weights). The liver and relative liver weights of Groups 6 and 8 were significantly smaller in comparison to Group 10. With respect to colon length, the value of Group 1 was significantly lower in comparison to Groups 6 ($p < 0.05$) and 7 ($p < 0.05$). The colon length of Group 3 was significantly larger in comparison to Group 1 ($p < 0.001$).

Pathological findings

Macroscopically, nodular and/or polypoid colonic tumors developed in the middle and distal colon of the mice in Groups 1–5. These tumors were histopathologically tubule adenoma (Fig.2*a*) or adenocarcinoma (well and moderately differentiated) (Fig. 2*b*) with a few adenocarcinomas that invaded into the serosa (Fig. 2*c*). A mucosal ulcer (Fig. 3*a*) was also observed surrounding the neoplasms. The enlarged lymph nodes with inflammation were present around the large bowel with tumors. The mice of Groups 6–10 had no tumors in all the organs examined, including the colon. A

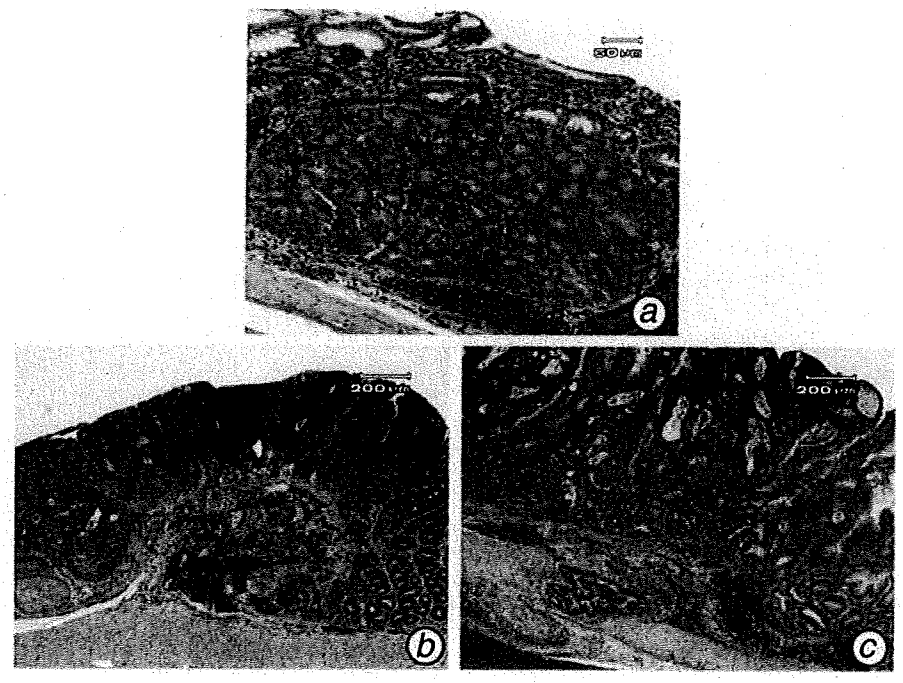

Figure 2. Representative colonic neoplasms induced by azoxymethane (AOM)/dextran sodium sulfate (DSS) in a mouse (Group 1). (*a*) A tubular adenoma, (*b*) a tubular adenocarcinoma with moderately differentiated and (*c*) a tubular adenocarcinoma invaded into the submucosa. Note: The severe inflammation around the tumors; Hematoxylin and eosin stain; the inserted bars indicate magnification (μm).

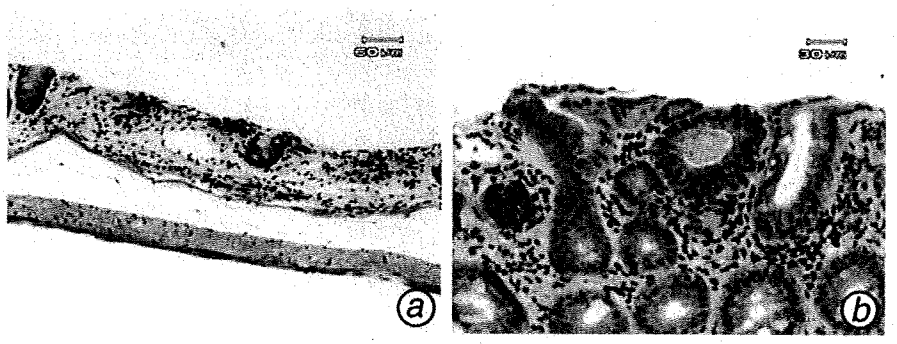

Figure 3. Representative colonic lesions induced by azoxymethane (AOM)/dextran sodium sulfate (DSS) in a mouse (Group 1). (*a*) Mucosal ulcer and (*b*) dysplastic crypts (circled). Hematoxylin and eosin stain, the inserted bars indicate magnification (μm).

mucosal ulcer was observed in the colon of some of the mice of Group 7.

The incidences and multiplicities of the colon neoplasms are summarized in Table 1. Group 1 (AOM/DSS) had 64% incidence of colonic adenocarcinoma with a multiplicity of 1.96 ± 2.24. The incidences of colonic adenocarcinoma of Groups 2 (AOM/DSS → 100 ppm GOFA/β-CD, 24%), 3 (AOM/DSS → 500 ppm GOFA/β-CD, 13%) and 5 (AOM/DSS → 500 ppm AUR/β-CD, 25%) were significantly smaller in comparison to Group 1 ($p < 0.005$, $p = 0.0001$ and $p < 0.005$, respectively). Also, the multiplicities of colonic adenocarcinoma of Groups 2 (0.52 ± 1.16, $p < 0.01$), 3 (0.25 ± 0.74, $p < 0.001$) and 5 (0.42 ± 0.83, $p < 0.05$) were significantly smaller in comparison to Group 1. The incidence (46%) and multiplicity (1.21 ± 1.61) of Group 4 (AOM/DSS → 100 ppm AUR/β-CD) were lower in comparison to Group 1, but the differences between the groups were insignificant. The incidences and multiplicities of colonic adenomas and total colonic tumors in Groups 2–5 were also lower in comparison to Group 1 (Table 1).

Table 1. Effects of compounds A and B on the development of colonic adenoma and adenocarcinoma

Group no.	Treatment	No. of mice examined	Incidence (%) AD	Incidence (%) ADC	Incidence (%) Total tumors (AD + ADC)	Multiplicity (no. of tumors/colon) AD	Multiplicity (no. of tumors/colon) ADC	Multiplicity (no. of tumors/colon) Total tumors (AD + ADC)
1	AOM[1]/1.5% DSS	28	61	64	71	1.39 ± 1.50[2]	1.96 ± 2.24	3.36 ± 3.34
2	AOM/1.5% DSS/100 ppm GOFA/β-CD	25	40	24[3]	40[4]	0.72 ± 1.06[5]	0.52 ± 1.16[5]	1.24 ± 2.11[6]
3	AOM/1.5% DSS/500 ppm GOFA/β-CD	24	25[7]	13[8]	29[3]	0.33 ± 0.64[6]	0.25 ± 0.74[9]	0.58 ± 1.21[9]
4	AOM/1.5% DSS/100 ppm AUR/β-CD	24	46	46	50	0.96 ± 1.27	1.21 ± 1.61	2.17 ± 2.81
5	AOM/1.5% DSS/500 ppm AUR/β-CD	24	50	25[3]	50	1.00 ± 1.32	0.42 ± 0.83[4]	1.42 ± 2.06[5]
6	AOM	5	0	0	0	0	0	0
7	1.5% DSS	5	0	0	0	0	0	0
8	500 ppm GOFA/β-CD	5	0	0	0	0	0	0
9	500 ppm AUR/β-CD	5	0	0	0	0	0	0
10	Untreated	5	0	0	0	0	0	0

[1]AOM, azoxymethane; DSS, dextran sodium sulfate; GOFA, 3-(4′-geranyloxy-3′-methoxyphenyl)-2-*trans* propenoic acid; CD, cyclodextrin; AUR, auraptene: AD, adenoma; ADC, adenocarcinoma. [2]Mean ± SD. [3]Significantly different from the AOM/DSS group (Group 1) by Chi-square test ($p < 0.005$). [4]Significantly different from the AOM/DSS group (Group 1) by Chi-square test ($p < 0.05$). [5]Significantly different from the AOM/DSS group (Group 1) by Turkey-Kramer multiple comparison post test ($p < 0.01$). [6]Significantly different from the AOM/DSS group (Group 1) by Turkey-Kramer multiple comparison post test ($p < 0.05$). [7]Significantly different from the AOM/DSS group (Group 1) by Chi-square test ($p < 0.01$). [8]Significantly different from the AOM/DSS group (Group 1) by Fisher's exact probability test ($p = 0.0001$). [9]Significantly different from the AOM/DSS group (Group 1) by Turkey-Kramer multiple comparison post test ($p < 0.001$).

Table 2. Effects of compounds A and B on colonic inflammation and development of mucosal ulcer and high-grade dysplasia

Group no.	Treatment	No. of mice examined	Inflammation score (incidence, %)	Number of colonic mucosal ulcer/colon (incidence)	No. of high-grade dysplasia/colon (incidence)
1	AOM[1]/1.5% DSS	28	2.79 ± 0.96[2]	1.29 ± 1.36 (75%)	2.21 ± 1.83 (82%)
2	AOM/1.5% DSS/100 ppm GOFA/β-CD	25	1.52 ± 1.05[3]	0.36 ± 0.64[4] (28%)	0.64 ± 1.19[4] (32%)
3	AOM/1.5% DSS/500 ppm GOFA/β-CD	24	0.75 ± 0.90[3]	0.33 ± 0.56[3] (29%)	0.50 ± 1.14[3] (25%)
4	AOM/1.5% DSS/100 ppm AUR/β-CD	24	1.71 ± 0.69[3]	0.42 ± 0.58[4] (38%)	1.25 ± 1.67 (50%)
5	AOM/1.5% DSS/500 ppm AUR/β-CD	24	1.17 ± 0.87[3]	0.33 ± 0.70[3] (21%)	0.75 ± 1.45[4] (33%)
6	AOM	5	0	0	0
7	1.5% DSS	5	2.20 ± 0.84	2.40 ± 0.89 (80%)	0
8	500 ppm GOFA/β-CD	5	0	0	0
9	500 ppm AUR/β-CD	5	0	0	0
10	Untreated	5	0	0	0

[1]AOM, azoxymethane; DSS, dextran sodium sulfate; GOFA, 3-(4′-geranyloxy-3′-methoxyphenyl)-2-*trans* propenoic acid; CD, cyclodextrin. [2]Mean ± SD. [3]Significantly different from the AOM/DSS group (Group 1) by Turkey-Kramer multiple comparison post test ($p < 0.001$). [4]Significantly different from the AOM/DSS group (Group 1) by Turkey-Kramer multiple comparison post test ($p < 0.01$).

Other colonic lesions, including colitis with or without mucosal ulcer (Fig. 3*a*) and cryptal dysplastia (Fig. 3*b*), were also observed in the colon of mice in Groups 1–5 and/or 7 (Table 2). With respect to the inflammation score (Table 2) determined on H&E-stained sections at Week 18, the value of Group 1 was the highest among the groups and the scores of Groups 2–5 were significantly smaller in comparison to Group 1 ($p < 0.001$ for each comparison). Similarly, as shown in Table 2, the number of colonic mucosal ulcer per colon of Group 1 was the greatest, and the values of Groups 2–5 were significantly smaller in comparison to Group 1 ($p < 0.01$ or $p < 0.001$). The inflammation score and number of mucosal ulcer of Group 7 were the second among the group. Colonic inflammation in the mice of Groups 6, 8, 9 and 10 was slight, if present, and there were mucosal ulcers in the colon of the mice belonging to these groups.

PCNA- and survivin-labeling index in the colonic adenocarcinomas

The data for the PCNA-, TUNEL- and survivin-positive rates of adenocarcinomas are illustrated in Figure 4. As shown in Figure 4*a*, the mean labeling indices of PCNA of Groups 2

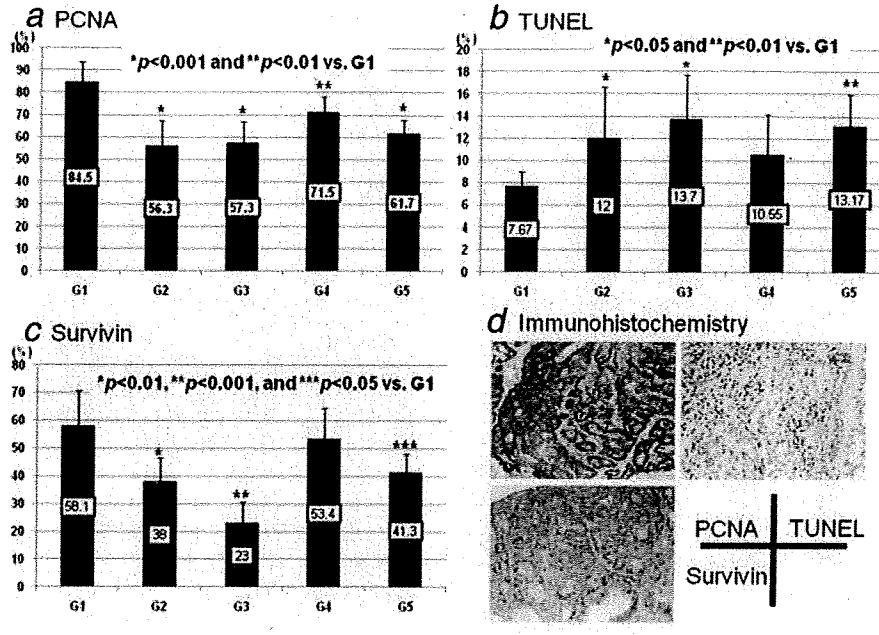

Figure 4. (*a*) The PCNA-labeling index (%, mean ± SD), (*b*) the TUNEL-positive rate (%, mean ± SD) and (*c*) the survivin-positive rate (%, mean ± SD) of colonic adenocarcinomas developed in mice from Groups 1–5. (*d*) The photos show representative PCNA-, TUNEL- and survivin-immunohistochemistry from Group 1.

(56.3 ± 11.2, $p < 0.001$), 3 (57.3 ± 9.6, $p < 0.001$), 4 (71.5 ± 9.4, $p < 0.01$) and 5 (61.7 ± 9.4, $p < 0.001$) were significantly lower in comparison to Group 1 (84.5 ± 9.4) (Fig. 4*d*). The mean TUNEL-positive rates of Groups 2 (12.00 ± 4.56, $p < 0.05$), 3 (13.70 ± 4.04, $p < 0.05$), 4 (10.55 ± 3.62) and 5 (13.17 ± 2.79, $p < 0.01$) were greater in comparison to Group 1 (7.67 ± 1.28) (Fig. 4*d*). With respect to the positive rates of survivin, the values of Groups 2 (38.0 ± 8.5, $p < 0.01$), 3 (23.0 ± 7.6, $p < 0.001$), 4 (53.4 ± 11.3) and 5 (41.3 ± 6.6, $p < 0.05$) were smaller in comparison to Group 1 (58.1 ± 12.6) (Fig. 4*d*).

Scores of NF-κB, Nrf2, Tnf-α, Stat3, IL-6 and IL-1β immunohistochemistry

The data for the scores of the immunohistochemical expression of these proinflammatory cytokines in colonic adenocarcinomas are illustrated in Figures 5*a*–5*c* and 6*a*–6*c*. Adenocarcinomas and the inflammatory mononuclear cells in the colon positively reacted with the antibodies of the proinflammatory cytokines, such as NF-κB, Nrf2, Tnf-α, Stat3, IL-6 and IL-1β (Figs. 5*d* and 6*d*). The scores of NF-κB (Fig. 5*a*), Stat3 (Fig. 6*a*), IL-6 (Fig. 6*b*) and IL-1β (Fig. 6*c*) of Groups 2–5 were significantly lower in comparison to Group 1. Similarly, the mean scores of Nrf2 (Fig. 5*b*) and Tnf-α (Fig. 5*c*) of Groups 2, 3 and 5 were significantly smaller in comparison to Group 1. Both values of Group 3 were lower in comparison to Group 1, but the differences were insignificant.

Discussion

The results of our study clearly indicated that the novel prodrugs, GOFA/β-CD and AUR/β-CD, effectively inhibited AOM/DSS-induced colitis-related colonic carcinogenesis without any adverse effects in mice. The effect of GOFA/β-CD was superior in comparison to AUR/β-CD. Dietary feeding with both prodrugs exerted their cancer chemopreventive ability by modulating cell proliferation, inducing apoptosis and suppressing the proinflammatory cytokines (NF-κB, Nrf2, Tnf-α, Stat3, IL-6 and IL-1β) in adenocarcinomas that developed in the inflamed colon. In turn, the expression of these cytokines may be involved in AOM/DSS-induced colon tumorigenesis. This is the first report showing that prodrugs of GOFA/β-CD and AUR/β-CD exert cancer chemopreventive ability in colitis-related colon carcinogenesis.

In our study, several proinflammatory cytokines were expressed in the colonic tumors and the inflammatory mononuclear cells infiltrated the tumors both internally and peripherally. As the expression of these cytokines may be involved in tumor growth,[52–54] we evaluated the effects of dietary GOFA/β-CD and AUR/β-CD on their expression in adenocarcinomas developed in Groups 1–5. The treatment with GOFA/β-CD and AUR/β-CD significantly lowered colonic inflammation induced by DSS. Chronic inflammation is involved in oncogenesis in certain tissues, including the large bowel. Therefore, the suppression of chronic inflammation through the modulation of expression of several

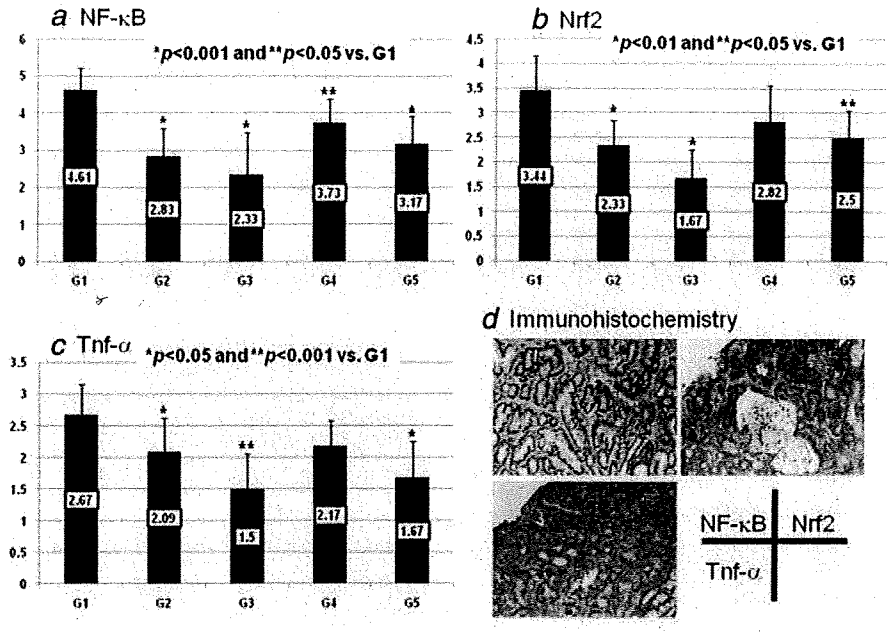

Figure 5. The scores (mean ± SD) of (*a*) NF-κB-, (*b*) Nrf2- and (*c*) Tnf-α-immunoreactivity of colonic adenocarcinomas developed in mice from Groups 1–5. (*d*) The photos show representative NF-κB-, Nrf2- and Tnf-α-immunohistochemistry from Group 1. Note: The adenocarcinoma cells strongly expressed NF-κB, Nrf2 and Tnf-α.

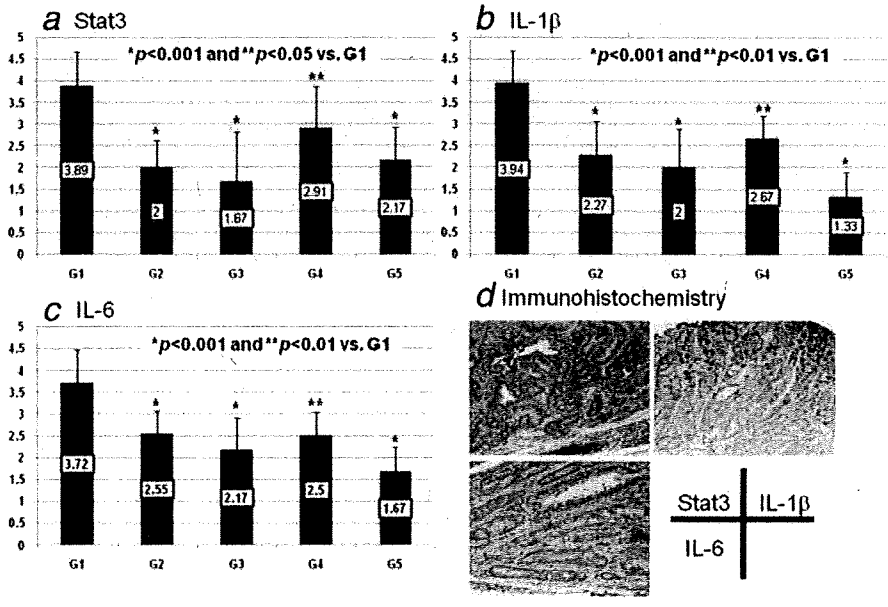

Figure 6. The scores (mean ± SD) of (*a*) Stat3-, (*b*) IL-1β- and (*c*) IL-6-immunoreactivity of colonic adenocarcinomas developed in the mice from Groups 1–5. (*d*) The photos show representative Stat3-, (*b*) IL-1b- and (*c*) IL-6-immunohistochemistry from Group 1. Note: The adenocarcinoma cells strongly expressed Stat3, IL-1β and IL-6.

proinflammatory gene products that mediate several events of carcinogenesis may result in cancer chemoprevention.[55] The modulation of inflammation and expression of cyclooxygenase (COX)-2 and inducible nitric oxide synthase (iNOS) in the colon results in the suppression of colitis-related colon carcinogenesis of mice.[56] Several molecular targets for the

suppression of inflammation-associated carcinogenesis were proposed.[36] In addition to the highly expressed levels of COX-2 and iNOS of colonic adenocarcinomas in our study (data not shown), the proinflammatory cytokines, such as NF-κB, Tnf-α, Stat3, Nrf2, IL-6 and IL-1β, were strongly expressed in adenocarcinomas that developed in the colon of the mice that received AOM and DSS. Moreover, dietary feeding with GOFA/β-CD and AUR/β-CD suppressed their expressions. The Nrf2-deficient mice are susceptible to DSS-induced colitis.[57] IL-6 and IL-1β are involved in the development of IBD and IBD-related colon cancer.[58,59] These proinflammatory cytokines are thus molecular targets for the chemoprevention of inflammation-related carcinogenesis.[31,37,55,60,61] They are candidate biomarkers of colon tumorigenesis,[62,63] because the expression of NF-κB, Tnf-α and IL-1β is involved in colonic tumorigenesis by affecting proliferation and apoptosis.[64–67] The activation of NF-κB, a transcription factor that is activated by several cytokines released during inflammation and is responsible for many of their proinflammatory effects, was shown to promote the growth of the colon tumors in experimental models.[31,55,60,68] Because of the strong link of NF-κB to different stress signals, including cigarette smoke, NF-κB has been called a "smoke-sensor" of the body.[69] In this context, the findings that a tobacco-specific carcinogen enhances AOM/DSS-induced colon carcinogenesis[70] are of interest. In addition, Stat3 expression is an important factor in colon carcinogenesis, tumor invasion[71] and survival/proliferation of the colonic preneoplastic cells.[72] In addition, the anti-inflammatory potential of melatonin through the suppression of the expression of NF-κB and chemokines (IL-8 and monocyte chemoattractant protein) in a rat colitis model[73,74] is of interest, and it is important to further investigate the cancer chemopreventive ability of this bioactive substance, as was done in our study.

In our study, the treatment with both compounds in the diet significantly lowered colonic inflammation induced by DSS. As chronic inflammation involves tumorigenesis and accelerate carcinogenic steps, the suppression of chronic inflammation through the modulation of the expression of several proinflammatory gene products that mediate a critical role in several events of carcinogenesis may result in the inhibition of cancer development, and it may also serve as cancer chemoprevention.[55] AUR and GOFA possess anti-inflammatory activities.[20,75] In addition, we previously reported on the cancer chemopreventive ability of AUR[22,76] and a prodrug, GOFA (called GAP in the study[23]) of the secondary metabolite of ferulic acid in colitis-associated colon carcinogenesis.[23,76] Several molecular targets for the suppression of inflammation-associated carcinogenesis were proposed.[36] Our recent study demonstrated that the modulation of inflammation and the expression of COX-2, iNOS and other proteins in the colon contribute to the suppression of colitis-related colon carcinogenesis.[10,56]

CDs (cyclic oligomers of glucose) that have the properties of forming inclusion complexes with lipophilic drugs have been widely used in therapy to improve water solubility and bioavailability of drugs. Target tissue bioavailability is an important determinant of these efficacies of chemopreventive agents.[77] In our study, we selected β-CD, which is soluble in water and organic solvents. When compared the chemopreventive efficacy of the inclusion complexes of GOFA and AUR with β-CD in our study to that of previous studies,[22,23] GOFA with β-CD was superior to GOFA[23] and AUR with β-CD was less effective in comparison to AUR.[22] This may be related to the differences between the thermal stability of GOFA/β-CD and AUR/β-CD. A thermogram of the AUR/β-CD complex showed that this coumarin derivative melting endotherm had a substantial reduction in peak area, thus implying that the molecular arrangement of AUR in the solid complex was different from the pure crystal compound.[25,27,45,46] Also, the different effects of these compounds with or without b-CD in the activity of matrix metalloproteinases of inflamed colon.[78]

In conclusion, the novel prodrugs of GOFA/β-CD and AUR/β-CD are effective in inhibiting colon cancer development in a two-stage colitis-related mouse colon carcinogenesis through modulation of inflammation, proliferation and the expression of several proinflammatory cytokines (NF-κB, Tnf-α, Stat3, Nrf2, IL-6 and IL-1β) in the inflamed colon of the mice that received AOM and DSS. Our findings therefore support the development of novel site-specifically delivered prodrugs for colon cancer prevention in the inflamed colon.

Acknowledgements

The authors thank Ms. Veronica Jimenez for the structural characterization of GOFA/β-CD and AUR/β-CD. This work was supported in part by a Grant-in-Aid (Nos. 18592076 to T.T., 17015016 to T.T. and 18880030 to Y.Y.) for Scientific Research from the Ministry of Education, Culture, Sports, Science and Technology of Japan and a grant (H2007-12 to T.T. and S2006-9 to Y.Y.) for the Project Research from the High-Technology Center of Kanazawa Medical University.

References

1. Parkin DM, Bray F, Ferlay J, Pisani P. Global cancer statistics, 2002. *CA Cancer J Clin* 2005;55:74–108.
2. WHO Media Center. Cancer fact sheet No. 297. WHO, 2006.
3. Tanaka T. Colorectal carcinogenesis: review of human and experimental animal studies. *J Carcinog* 2009;8:5.
4. Balkwill F, Mantovani A. Inflammation and cancer: back to Virchow? *Lancet* 2001; 357:539–45.
5. Rubin DT, Parekh N. Colorectal cancer in inflammatory bowel disease: molecular and clinical considerations. *Curr Treat Options Gastroenterol* 2006;9: 211–20.
6. Tanaka T, Kohno H, Murakami M, Shimada R, Kagami S. Colitis-related rat colon carcinogenesis induced by 1-hydroxy-anthraquinone and methylazoxymethanol acetate (review). *Oncol Rep* 2000;7:501–8.
7. Tanaka T, Kohno H, Suzuki R, Yamada Y, Sugie S, Mori H. A novel inflammation-

related mouse colon carcinogenesis model induced by azoxymethane and dextran sodium sulfate. *Cancer Sci* 2003;94:965–73.
8. Suzuki R, Kohno H, Sugie S, Nakagama H, Tanaka T. Strain differences in the susceptibility to azoxymethane and dextran sodium sulfate-induced colon carcinogenesis in mice. *Carcinogenesis* 2006;27:162–9.
9. Suzuki R, Kohno H, Sugie S, Tanaka T. Sequential observations on the occurrence of preneoplastic and neoplastic lesions in mouse colon treated with azoxymethane and dextran sodium sulfate. *Cancer Sci* 2004;95:721–7.
10. Suzuki R, Miyamoto S, Yasui Y, Sugie S, Tanaka T. Global gene expression analysis of the mouse colonic mucosa treated with azoxymethane and dextran sodium sulfate. *BMC Cancer* 2007;7:84.
11. Kohno H, Suzuki R, Curini M, Epifano F, Maltese F, Gonzales SP, Tanaka T. Dietary administration with prenyloxycoumarins, auraptene and collinin, inhibits colitis-related colon carcinogenesis in mice. *Int J Cancer* 2006;118:29336–42.
12. Kohno H, Suzuki R, Yasui Y, Miyamoto S, Wakabayashi K, Tanaka T. Ursodeoxycholic acid versus sulfasalazine in colitis-related colon carcinogenesis in mice. *Clin Cancer Res* 2007;13:2519–25.
13. Kohno H, Suzuki R, Sugie S, Tanaka T. Beta-catenin mutations in a mouse model of inflammation-related colon carcinogenesis induced by 1,2-dimethylhydrazine and dextran sodium sulfate. *Cancer Sci* 2005;2005:69–76.
14. Tanaka T, Suzuki R, Kohno H, Sugie S, Takahashi M, Wakabayashi K. Colonic adenocarcinomas rapidly induced by the combined treatment with 2-amino-1-methyl-6-phenylimidazo[4,5-*b*]pyridine and dextran sodium sulfate in male ICR mice possess beta-catenin gene mutations and increases immunoreactivity for beta-catenin, cyclooxygenase-2 and inducible nitric oxide synthase. *Carcinogenesis* 2005;26:229–38.
15. Tanaka T, Kohno H, Suzuki R, Hata K, Sugie S, Niho N, Sakano K, Takahashi M, Wakabayashi K. Dextran sodium sulfate strongly promotes colorectal carcinogenesis in Apc(Min/+) mice: inflammatory stimuli by dextran sodium sulfate results in development of multiple colonic neoplasms. *Int J Cancer* 2006;118:25–34.
16. Ohshima H, Tazawa H, Sylla BS, Sawa T. Prevention of human cancer by modulation of chronic inflammatory processes. *Mutat Res* 2005;591:110–22.
17. D'Inca R, Cardin R, Benazzato L, Angriman I, Martines D, Sturniolo GC. Oxidative DNA damage in the mucosa of ulcerative colitis increases with disease duration and dysplasia. *Inflamm Bowel Dis* 2004;10:23–7.
18. Papadakis KA, Targan SR. Role of cytokines in the pathogenesis of inflammatory bowel disease. *Annu Rev Med* 2000;51:289–98.
19. Rutgeerts P, Vermeire S, Van Assche G. Biological therapies for inflammatory bowel diseases. *Gastroenterology* 2009;136:1182–97.
20. Tanaka T, Yasui Y, Ishigamori-Suzuki R, Oyama T. Citrus compounds inhibit inflammation- and obesity-related colon carcinogenesis in mice. *Nutr Cancer* 2008;60(Suppl 1):70–80.
21. Tanaka T, Yasui Y, Tanaka M, Oyama T, Rahman KM. Melatonin suppresses AOM/DSS-induced large bowel oncogenesis in rats. *Chem Biol Interact* 2009;177:128–36.
22. Kohno H, Suzuki R, Curini M, Epifano F, Maltese F, Gonzales SP, Tanaka T. Dietary administration with prenyloxycoumarins, auraptene and collinin, inhibits colitis-related colon carcinogenesis in mice. *Int J Cancer* 2006;118:2936–42.
23. Miyamoto S, Epifano F, Curini M, Genovese S, Kimi M, Ishigamori-Suzuki R, Yasui Y, Sugie S, Tanaka T. A novel prodrug of 4′-geranyloxy-ferulic acid suppresses colitis-related colon carcinogenesis in mice. *Nutr Cancer* 2008;60:675–84.
24. Loftsson T, Duchêne D. Cyclodextrins and their pharmaceutical applications. *Int J Pharm* 2007;329:1–11.
25. De Azevedo MBM, Alderete JB, Lino ACS, Loh W, Faljoni-Alario A, Duran N. Violacein/β-cyclodextrin inclusion complex formation studied by measurements of diffusion coefficient and circular dichroism. *J Inclusion Phenom Macrocycl Chem* 2000;37:67–74.
26. De Azevedo MBM, Correa DHA, Carvalho CAA, Haun M, Duran N, Melo PS. Dehydrocrotonin and its β-cyclodextrin complex: cytotoxicity in V79 fibroblasts and rat cultured hepatocytes. *Eur J Pharmacol* 2005;510:17–24.
27. De Azevedo MBM, Melo PS, Justo GZ, Duran N, Haun M. Violacein and its β-cyclodextrin complexes induce apoptosis and differentiation in HL60 cells. *Toxicology* 2003;186:217–25.
28. Meissner Y, Lamprecht A. Alternative drug delivery approaches for the therapy of inflammatory bowel disease. *J Pharm Sci* 2008;97:2878–91.
29. Curini M, Epifano F, Genovese S, Marcotullio MC, Menghini L. 3-(4′-Geranyloxy-3′-Methoxyphenyl)-2-trans propenoic acid: a novel promising cancer chemopreventive agent. *Anticancer Agents Med Chem* 2006;6:571–7.
30. Epifano F, Genovese S, Curini M. Auraptene: phytochemical and pharmacological properties. In: Matsumoto T, editor. Phytochemistry research progressed. Hauppauge, NY: Nova Science Publishers, 2008.145–62.
31. Surh YJ. NF-kappa B and Nrf2 as potential chemopreventive targets of some anti-inflammatory and antioxidative phytonutrients with anti-inflammatory and antioxidative activities. *Asia Pac J Clin Nutr* 2008;17(Suppl 1):269–72.
32. Sarkar FH, Li Y. NF-kappaB: a potential target for cancer chemoprevention and therapy. *Front Biosci* 2008;13:2950–9.
33. Bharti AC, Aggarwal BB. Nuclear factor-kappa B and cancer: its role in prevention and therapy. *Biochem Pharmacol* 2002;64:883–8.
34. Kwon KH, Barve A, Yu S, Huang MT, Kong AN. Cancer chemoprevention by phytochemicals: potential molecular targets, biomarkers and animal models. *Acta Pharmacol Sin* 2007;28:1409–21.
35. Aggarwal BB, Sethi G, Baladandayuthapani V, Krishnan S, Shishodia S. Targeting cell signaling pathways for drug discovery: an old lock needs a new key. *J. Cell Biochem* 2007;102:580–92.
36. Aggarwal BB, Shishodia S. Molecular targets of dietary agents for prevention and therapy of cancer. *Biochem Pharmacol* 2006;71:1397–421.
37. Sethi G, Sung B, Aggarwal BB. TNF: a master switch for inflammation to cancer. *Front Biosci* 2008;13:5094–107.
38. Atreya R, Neurath MF. Signaling molecules: the pathogenic role of the IL-6/STAT-3 trans signaling pathway in intestinal inflammation and in colonic cancer. *Curr Drug Targets* 2008;9:369–74.
39. Mitsuyama K, Matsumoto S, Masuda J, Yamasakii H, Kuwaki K, Takedatsu H, Sata M. Therapeutic strategies for targeting the IL-6/STAT3 cytokine signaling pathway in inflammatory bowel disease. *Anticancer Res* 2007;27:3749–56.
40. Kwon KH, Murakami A, Hayashi R, Ohigashi H. Interleukin-1beta targets interleukin-6 in progressing dextran sulfate sodium-induced experimental colitis. *Biochem Biophys Res Commun* 2005;337:647–54.
41. Kim M, Miyamoto S, Yasui Y, Oyama T, Murakami A, Tanaka T. Zerumbone, a tropical ginger sesquiterpene, inhibits colon and lung carcinogenesis in mice. *Int J Cancer* 2009;124:264–71.
42. Watson AJ. An overview of apoptosis and the prevention of colorectal cancer. *Crit Rev Oncol Hematol* 2006;57:107–21.
43. Curini M, Epifano F, Genovese S. Synthesis of a novel prodrug of 3-(4′-geranyloxy-3′-methoxyphenyl)-2-trans-propenoic acid for colon delivery. *Bioorg Med Chem Lett* 2005;15:5049–52.

44. Curini M, Epifano F, Maltese F, Marcotullio MC, Tubaro A, Altinier G, Prieto Gonzales S, Rodriguez JC. Synthesis and anti-inflammatory activity of natural and semisynthetic geranyloxycoumarins. *Bioorg Med Chem Lett* 2004;14:2241–3.
45. De Azevedo MBM, Alderete J, Rodriguez JA, Souza AO, Rettori D, Torsoni MA, Faljoni-Alario A, Haun M, Duran N. Biological activities of violacein, a new antitumoral indole derivative, in an inclusion complex with beta-cyclodextrin. *J Inclusion Phenom Macrocycl Chem* 2000;37:93–101.
46. De Azevedo MBM, Zullo MAT, Alderete JB, De Azevedo MMM, Salva TJG, Duran N. Characterisation and properties of the inclusion complex of 24-epibrassinolide with beta-cyclodextrin. *Plant Growth Reg* 2002;37:233–40.
47. Carino SR, Tostmann H, Underhill RS, Logan J, Weerasekera G, Culp J, Davidson M, Duran RS. Real-time grazing incidence X-ray diffraction studies of polymerizing *N*-octadecyltrimethoxysilane Langmuir monolayers at the air/water interface. *J Am Chem Soc* 2001;123:767–8.
48. De Azevedo MBM, Duran N, Justo GZ, Melo PS, Brito ARMS, Almeida ABA, Haun M. Evaluation of the antiulcerogenic activity of violacein and its modulation by the inclusion complexation with beta-cyclodextrin. *Can J Physiol Pharmacol* 2003;81:387–96.
49. De Souza AO, Alderete JB, Faljoni-Alario A, Silva CL, Duran N. Physico-chemical characterization of the inclusion complex between a 2-propen-1-amine derivative and beta-cyclodextrin. *J Chil Chem Soc* 2005;50: 591–6.
50. Ward JM. Morphogenesis of chemically induced neoplasms of the colon and small intestine in rats. *Lab Invest* 1974;30: 505–13.
51. Yasui Y, Suzuki R, Miyamoto S, Tsukamoto T, Sugie S, Kohno H, Tanaka T. A lipophilic statin, pitavastatin, suppresses inflammation-associated mouse colon carcinogenesis. *Int J Cancer* 2007; 121: 2331–9.
52. Lewis AM, Varghese S, Xu H, Alexander HR. Interleukin-1 and cancer progression: the emerging role of interleukin-1 receptor antagonist as a novel therapeutic agent in cancer treatment. *J Transl Med* 2006;4:48.
53. Lin WW, Karin M. A cytokine-mediated link between innate immunity, inflammation, and cancer. *J Clin Invest* 2007;117:1175–83.
54. Yoo SY, Lee SY, Yoo NC. Cytokine expression and cancer detection. *Med Sci Monit* 2009;15:RA49–56.
55. Aggarwal BB, Shishodia S, Sandur SK, Pandey MK, Sethi G. Inflammation and cancer: how hot is the link? *Biochem Pharmacol* 2006;72:1605–21.
56. Kohno H, Suzuki R, Sugie S, Tanaka T. Suppression of colitis-related mouse colon carcinogenesis by a COX-2 inhibitor and PPAR ligands. *BMC Cancer* 2005;5:46.
57. Khor TO, Huang MT, Kwon KH, Chan JY, Reddy BS, Kong AN. Nrf2-deficient mice have an increased susceptibility to dextran sulfate sodium-induced colitis. *Cancer Res* 2006;66:11580–4.
58. Atreya R, Neurath MF. Involvement of IL-6 in the pathogenesis of inflammatory bowel disease and colon cancer. *Clin Rev Allergy Immunol* 2005;28:187–96.
59. Hanai H. Positions of selective leukocytapheresis in the medical therapy of ulcerative colitis. *World J Gastroenterol* 2006;12:7568–77.
60. Surh YJ, Na HK. NF-kappaB and Nrf2 as prime molecular targets for chemoprevention and cytoprotection with anti-inflammatory and antioxidant phytochemicals. *Genes Nutr* 2008;2:313–17.
61. Kim YS, Young MR, Bobe G, Colburn NH, Milner JA. Bioactive food components, inflammatory targets, and cancer prevention. *Cancer Prev Res* 2009;2:200–8.
62. Janakiram NB, Rao CV. Molecular markers and targets for colorectal cancer prevention. *Acta Pharmacol Sin* 2008;29: 1–20.
63. Yasui Y, Kim M, Tanaka T. Colorectal carcinogenesis and suppression of tumor development by inhibition of enzymes and molecular targets. *Curr Enzyme Inhibit* 2009;5:1–26.
64. Dong M, Guda K, Nambiar PR, Rezaie A, Belinsky GS, Lambeau G, Giardina C, Rosenberg DW. Inverse association between phospholipase A2 and COX-2 expression during mouse colon tumorigenesis. *Carcinogenesis* 2003;24:307–15.
65. Inan MS, Place R, Tolmacheva V, Wang QS, Hubbard AK, Rosenberg DW, Giardina C. IkappaBbeta-related proteins in normal and transformed colonic epithelial cells. *Mol Carcinog* 2000;29:25–36.
66. Inan MS, Tolmacheva V, Wang QS, Rosenberg DW, Giardina C. Transcription factor NF-kappaB participates in regulation of epithelial cell turnover in the colon. *Am J Physiol Gastrointest Liver Physiol* 2000; 279:G1282–G1291.
67. Tong X, Yin L, Washington R, Rosenberg DW, Giardina C. The p50-p50 NF-kappaB complex as a stimulus-specific repressor of gene activation. *Mol Cell Biochem* 2004; 265:171–83.
68. Fantini MC, Pallone F. Cytokines: from gut inflammation to colorectal cancer. *Curr Drug Targets* 2008;9:375–80.
69. Ahn KS, Aggarwal BB. Transcription factor NF-kappaB: a sensor for smoke and stress signals. *Ann N Y Acad Sci* 2005;1056: 218–33.
70. Kim M, Miyamoto S, Sugie S, Yasui Y, Ishigamori-Suzuki R, Murakami A, Nakagama H, Tanaka T. A tobacco-specific carcinogen, NNK, enhances AOM/DSS-induced colon carcinogenesis in male A/J mice. *In Vivo* 2008;22:557–63.
71. Kusaba T, Nakayama T, Yamazumi K, Yakata Y, Yoshizaki A, Nagayasu T, Sekine I. Expression of p-STAT3 in human colorectal adenocarcinoma and adenoma: correlation with clinicopathological factors. *J Clin Pathol* 2005;58:833–8.
72. Fenton JI, Hursting SD, Perkins SN, Hord NG. Interleukin-6 production by leptin treatment promotes cell proliferation in an Apc(Min/+) colon epithelial cell line. *Carcinogenesis* 2006;27:1507–15.
73. Li JH, Yu JP, Yu HG, Xu XM, Yu LL, Liu J, Luo HS. Melatonin reduces inflammatory injury through inhibiting NF-kappaB activation in rats with colitis. *Mediators Inflamm* 2005;2005:185–93.
74. Li JH, Zhou W, Liu K, Li HX, Wang L. Melatonin reduces the expression of chemokines in rat with trinitrobenzene sulfonic acid-induced colitis. *Saudi Med J* 2008;29:1088–94.
75. Epifano F, Genovese S, Sosa S, Tubaro A, Curini M. Synthesis and anti-inflammatory activity of 3-(4′-geranyloxy-3′-methoxyphenyl)-2-trans propenoic acid and its ester derivatives. *Bioorg Med Chem Lett* 2007;17:5709–14.
76. Tanaka T, Kawabata K, Kakumoto M, Hara A, Murakami A, Kuki W, Takahashi Y, Yonei H, Maeda M, Ota T, Odashima S, Yamane T, et al. Citrus auraptene exerts dose-dependent chemopreventive activity in rat large bowel tumorigenesis: the inhibition correlates with suppression of cell proliferation and lipid peroxidation and with induction of phase II drug-metabolizing enzymes. *Cancer Res* 1998;58: 2550–6.
77. Boukharta M, Jalbert G, Castonguay A. Biodistribution of ellagic acid and dose-related inhibition of lung tumorigenesis in A/J mice. *Nutr Cancer* 1992;18:181–9.
78. Kawabata K, Murakami A, Ohigashi H. Auraptene decreases the activity of matrix metalloproteinases in dextran sulfate sodium-induced ulcerative colitis in ICR mice. *Biosci Biotechnol Biochem* 2006;70: 3062–5.

Methylation Silencing of Transforming Growth Factor-β Receptor Type II in Rat Prostate Cancers

Satoshi Yamashita,[1] Satoru Takahashi,[2] Nathalie McDonell,[1] Naoko Watanabe,[1] Tohru Niwa,[1] Kosuke Hosoya,[1] Yoshimi Tsujino,[1] Tomoyuki Shirai,[2] and Toshikazu Ushijima[1]

[1]Carcinogenesis Division, National Cancer Center Research Institute, Chuo-ku, Tokyo, Japan and [2]Department of Experimental Pathology and Tumor Biology, Nagoya City University Graduate School of Medical Sciences, Mizuho-ku, Nagoya, Japan

Abstract

To identify methylation-silenced genes in prostate cancers, a microarray analysis for genes up-regulated by treatment with a demethylating agent, 5-aza-2′-deoxycytidine, was performed using three rat prostate cancer cell lines. Eight genes (*Aebp1, Dysf, Gas6, LOC361288, Nnat, Ocm, RGD1308119*, and *Tgfbr2*) were re-expressed at 16-fold or more, and their promoter CpG islands were shown to be densely methylated in the cancer cell lines. From the eight genes, *Tgfbr2*, a key mediator of transforming growth factor-β (TGF-β) signaling that has been strongly implicated in human and rat prostate carcinogenesis, was selected, and its silencing in primary samples was analyzed further. *Tgfbr2* was methylated and markedly down-regulated in three of seven 3,2′-dimethyl-4-aminobiphenyl–induced invasive adenocarcinomas in the dorsolateral lobe of the rat prostate. In humans, marked down-regulation of TGFBR2 protein was observed in 12 of 20 high-grade prostatic intraepithelial neoplasia and 36 of 60 prostate cancers. DNA methylation of the human *TGFBR2* promoter CpG islands repressed transcription, if present, but neither methylation nor mutation were detected in 27 human prostate cancers analyzed. Methylation silencing of rat *Tgfbr2* was associated with histone H3 lysine 9 trimethylation, whereas decreased expression of human *TGFBR2* was mainly due to decreased transcription activity, sometimes in concert with histone deacetylation and H3 lysine 27 trimethylation. The identification of methylation silencing of *Tgfbr2* in rat prostate cancers, in accordance with *TGFBR2* down-regulation in human prostate cancers, will enable us to analyze how aberrant methylation is induced *in vivo* and identify factors that promote and suppress the induction of aberrant methylation. [Cancer Res 2008;68(7):2112–21]

Introduction

Gene silencing due to DNA methylation of promoter CpG islands (CGIs) is one of the major mechanisms of tumor-suppressor gene inactivation, along with mutations and loss of heterozygosity (1). Many methylation-silenced tumor-suppressor genes have been identified, and more will be revealed by genome-wide procedures (2). In contrast, limited information is available on the mechanism of how methylation silencing is induced *in vivo* and on the factors that promote or suppress aberrant methylation. For example, although chronic inflammation is known to be an inducer of aberrant methylation in humans (3), the exact effector cells and molecular changes in target cells are unknown. To address these questions, animal models are indispensable. However, because we select models by the presence of dense methylation of a promoter CGI in cancer and by the meaningful expression of its downstream gene in the corresponding normal tissue, only a limited number of methylation-silenced genes have thus far been identified in animal models (4–7).

Prostate cancer is one of the leading causes of cancer death in men in most developed countries (8). To analyze molecular, cellular, and physiologic events in prostate carcinogenesis, rodent models have been used. Particularly in rats, prostate cancers can be induced in an age-dependent manner in ACI/Seg and Lobound-Wistar strains, or by chemical carcinogens, and the effects of androgens have been clearly shown (9). If methylation-silenced genes involved in prostate carcinogenesis are found in rat prostate cancers, they will enable us to analyze the molecular processes of how aberrant methylation is induced *in vivo* as well as the factors, including hormones, that influence the process.

To identify methylation-silenced genes in rat prostate cancers, a chemical genomic screening method (2) was adopted for its efficiency. This method screens genes re-expressed after treatment with the demethylating agent 5-aza-2′-deoxycytidine (5-aza-dC), using a microarray. It is technically simple, and effective in identifying methylation-silenced genes using cell lines. Three rat prostate cancer cell lines, PLS10, PLS20, and PLS30 have been established from three prostate cancers in the dorsolateral lobes independently induced by 3,2′-dimethyl-4-aminobiphenyl (DMAB) plus testosterone in male F344 rats (10, 11).

Here, we report the results of a chemical genomic screening using PLS10, PLS20, and PLS30 cell lines. Among the genes whose methylation silencing was confirmed, the transforming growth factor-β (TGF-β) receptor type II gene (*Tgfbr2*), a key mediator of TGF-β signaling that has been strongly implicated in human and rat prostate carcinogenesis (12–19), was identified. We further analyzed *Tgfbr2* methylation and expression both in rat and human prostate cancers.

Materials and Methods

Cell lines and their 5-aza-dC or trichostatin A treatment. PLS10 (well-differentiated adenocarcinoma), PLS20 (poorly differentiated adenocarcinoma), and PLS30 (well-differentiated adenocarcinoma) were established from three independent transplantable tumor lines induced by DMAB plus testosterone propionate in the dorsolateral lobes of F344 rats, and maintained as reported (11). Human prostate cancer cell lines (PC3, LNCaP, DU145, MDA-PCa-2b, and 22Rv1) and prostatic epithelial cells immortalized by papillomavirus 18 (RWPE-1) were purchased from the American Type Culture Collection.

Note: Supplementary data for this article are available at Cancer Research Online (http://cancerres.aacrjournals.org).

Requests for reprints: Toshikazu Ushijima, Carcinogenesis Division, National Cancer Center Research Institute, 1-1 Tsukiji 5-chome, Chuo-ku, Tokyo 104-0045, Japan. Phone: 81-3-3542-2511; Fax: 81-3-5565-1753; E-mail: tushijim@ncc.go.jp.

doi:10.1158/0008-5472.CAN-07-5282

Table 1. Eight genes silenced in rat prostate cancer cell lines

Gene symbol	CpG island (bp)	Methylation and expression induction			Gene title
		PLS-10	PLS-20	PLS-30	
Aebp1	500	M*	M	M	AE binding protein 1 (predicted)
Dysf	300	M	M*	M	Dysferlin (predicted)
Gas6	500	M*	M	M†	Growth arrest–specific 6
LOC361288	500	M*	U	U	Similar to FUN14 domain containing 2 (predicted)
Nnat	500	M*	M†	M†	Neuronatin
Ocm	300	M*	M*	M/U*	Oncomodulin
RGD1308119	500	M*	M	M	Similar to F-box protein FBL2
Tgfbr2	500	M/U	M*	M†	TGF-β receptor II

Abbreviations: M, methylated; U, unmethylated.
*≥16-fold increase.
† ≥4-fold increase.

For treatment with 5-aza-dC, 2×10^5 cells (1×10^5 cells for PLS-10)/10 cm dish were seeded on day 0, and exposed to freshly prepared 10 μmol/L 5-aza-dC (Sigma) for 24 h on days 1 and 3. This dose suppressed cellular growth rates to approximately half of nontreated cells. After each treatment, the cells were placed in fresh medium and harvested on day 4. For treatment with trichostatin A (TSA), cells were seeded at a half-confluent density, and exposed to 100, 300, and 1,000 nmol/L of TSA (Sigma) for 24 h until harvest. Genomic DNA was extracted by standard phenol/chloroform procedures. Total RNA was extracted using ISOGEN (Nippon Gene) and purified using an RNeasy Mini kit (Qiagen).

Primary prostate cancers and immunohistochemistry. To induce prostate cancers, 6-week-old male F344 rats underwent subcutaneous injection of 100 mg/kg of testosterone propionate and 50 mg/kg of DMAB, which was repeated 10 times in a 2-week cycle, followed by the subcutaneous implantation of a Silastic tube containing 40 mg of testosterone propionate (10). The prostate was resected *en bloc*, examined for gross abnormalities, and fixed in 10% buffered formalin. One sagittal slice was prepared for each lobe, and embedded in paraffin. A 4-μm-thick section was stained with H&E. Organ-confined prostate cancers were obtained from 60 patients (ages 49–77, stage II–IV, Gleason pattern 2–5) who underwent prostatectomy. None of these cancer patients had previously undergone chemotherapy, radiotherapy, or hormonal therapy. All histologic diagnoses were made by experienced pathologists (S. Takahashi and T. Shirai). DNA from formalin-fixed, paraffin-embedded tissue sections was extracted by heating the sections at 100°C for 20 min under pH 12 (20). The animal experiment protocols were approved by the Committee for Ethics in Animal Experimentation at the National Cancer Center.

TGFBR2 immunohistochemistry in rat and human prostate cancers was performed using polyclonal anti-TGFBR2 antibody (L-21, Santa Cruz Biotechnology). The areas with TGFBR2 protein expression were quantitatively measured by an Image Processor for Analytical Pathology (IPAP-WIN, Sumika Technoservice), and regions that had an absorbance of one-third or less of the normal prostate were considered to have TGFBR2 down-regulation.

Oligonucleotide microarray analysis and database search. Oligonucleotide microarray analysis was performed using a GeneChip Rat Genome 230 2.0 Array (Affymetrix) and GeneChip Operating Software as in our previous studies (21, 22). Database searches were carried out at a GenBank web site, and CGI were searched for based on (*a*) CpG score ≥ 0.65, (*b*) G + C content ≥ 55%, and (*c*) length (≥200, ≥300, or ≥500 bp).

Methylation-specific PCR and bisulfite sequencing. DNA from cell lines was digested by *Bam*HI and 1 μg of digested DNA was denatured in 0.3 N NaOH at 37°C for 15 min. DNA from formalin-fixed, paraffin-embedded tissue sections was used without digestion (0.2–0.5 μg each). The samples in 3.6 N sodium bisulfite (pH 5.0) and 0.6 mmol/L of hydroquinone underwent 15 cycles of 30-s denaturation at 95°C and 15-min incubation at 50°C, desalted and desulfonated with Zymo-Spin IC Columns (Zymo Research), and were dissolved in 16 to 40 μL of TE buffer.

Methylation-specific PCR (MSP) was performed with a primer set specific to the methylated or unmethylated sequence (M or U set), using 0.5 μL (2.0 μL for DNA from formalin-fixed tissue) of the sodium bisulfite–treated DNA. DNA methylated with *Sss*I methylase (New England Biolabs) and DNA amplified by a GenomiPhi DNA amplification kit (GE Healthcare Bio-Sciences) was used as fully methylated and unmethylated control DNA, respectively (23). Bisulfite sequencing was performed with primers common to methylated and unmethylated DNA sequences, using 0.5 μL (1.0 μL for DNA from formalin-fixed tissue) of the sodium bisulfite–treated DNA (22). Primer sequences are shown in Supplementary Table S1.

Quantitative reverse transcription-PCR and 5′-rapid amplification of cDNA ends. cDNA was synthesized from 1 μg of total RNA using a QuantiTect Reverse Transcription Kit (Qiagen) with a random primer. Real-time PCR was performed using the 7300 Real-Time PCR System (Applied Biosystems) with SYBR Green Real-Time PCR Master Mix (Toyobo; ref. 22). The copy number of a target gene was normalized to that of *GAPDH* in human and cyclophilin A (*Ppia*) in rat (24). Primer sequences are shown in Supplementary Table S2.

Rapid amplification of 5′ complementary DNA ends (5′ RACE) was performed using a GeneRacer kit (Invitrogen) on cDNA from AT6.3 and MAT-LyLu rat prostate cancer cell lines that abundantly expressed *Tgfbr2*. After the first and second PCR using LA Taq (Takara Bio), the PCR product was cloned into a pGEM-T Easy Vector (Promega), and a total of 54 clones were sequenced using a DYEnamic ET Terminator Cycle Sequencing Kit (GE Healthcare Bio-Sciences) and an ABI310 DNA sequencer (Applied Biosystems).

Chromatin immunoprecipitation analysis. Cells (1.5×10^6) were treated with 1% formaldehyde for 10 min at room temperature for cross-linking, and the reaction was quenched by adding glycine. Cells were lysed in the SDS lysis buffer containing protease inhibitors (Upstate), and DNA was sonicated to a size of 100 to 3,000 bp by Bioruptor UCD-250 (Cosmo Bio). To the sonicated solution, anti-K4 dimethylated histone H3 (H3K4me2, Upstate), anti-K9 trimethylated histone H3 (H3K9me3, Upstate), or anti-K27 trimethylated histone H3 (H3K27me3, Upstate) was added, and the mixture was incubated at 4°C overnight with rotation. The resultant immune complexes were collected using Dynabeads protein G (Invitrogen Dynal AS), and washed with Immune Complex Wash Buffer (Upstate). The cross-link was reversed by incubation for 5 h at 65°C in the presence of 0.3 mol/L of NaCl. DNA was recovered by treatment with RNase and proteinase K,

phenol/chloroform extraction, and isopropanol precipitation. The number of DNA molecules precipitated from a specific starting volume of the sonicated solution was compared with the number of DNA molecules in the same volume of the sonicated solution (whole cell extract). The number of DNA molecules was quantified by real-time PCR (primer sequences in Supplementary Table S1).

Luciferase reporter assay using a promoter with DNA methylation of a specific region. The 5′ region of human *TGFBR2* was amplified using an upper primer (5′-CCAGGAATGTCTTGGGCAAA-3′) and a lower primer (5′-CCAGCGCAGCGGACG-3′) and cloned into a *Sma*I site of the pGL3-Basic vector (Promega). To methylate a specific region within the reporter plasmid, the region was excised and methylated twice by *Sss*I methylase. The methylated DNA fragment and the mock-treated DNA fragment (treatment without *S*-adenosylmethionine) were ligated back into the remaining arm using Ligation high (Toyobo). Nonessential regions within the reporter plasmid were digested with *Sac*I, *Bam*HI, and *Fsp*I. Then,

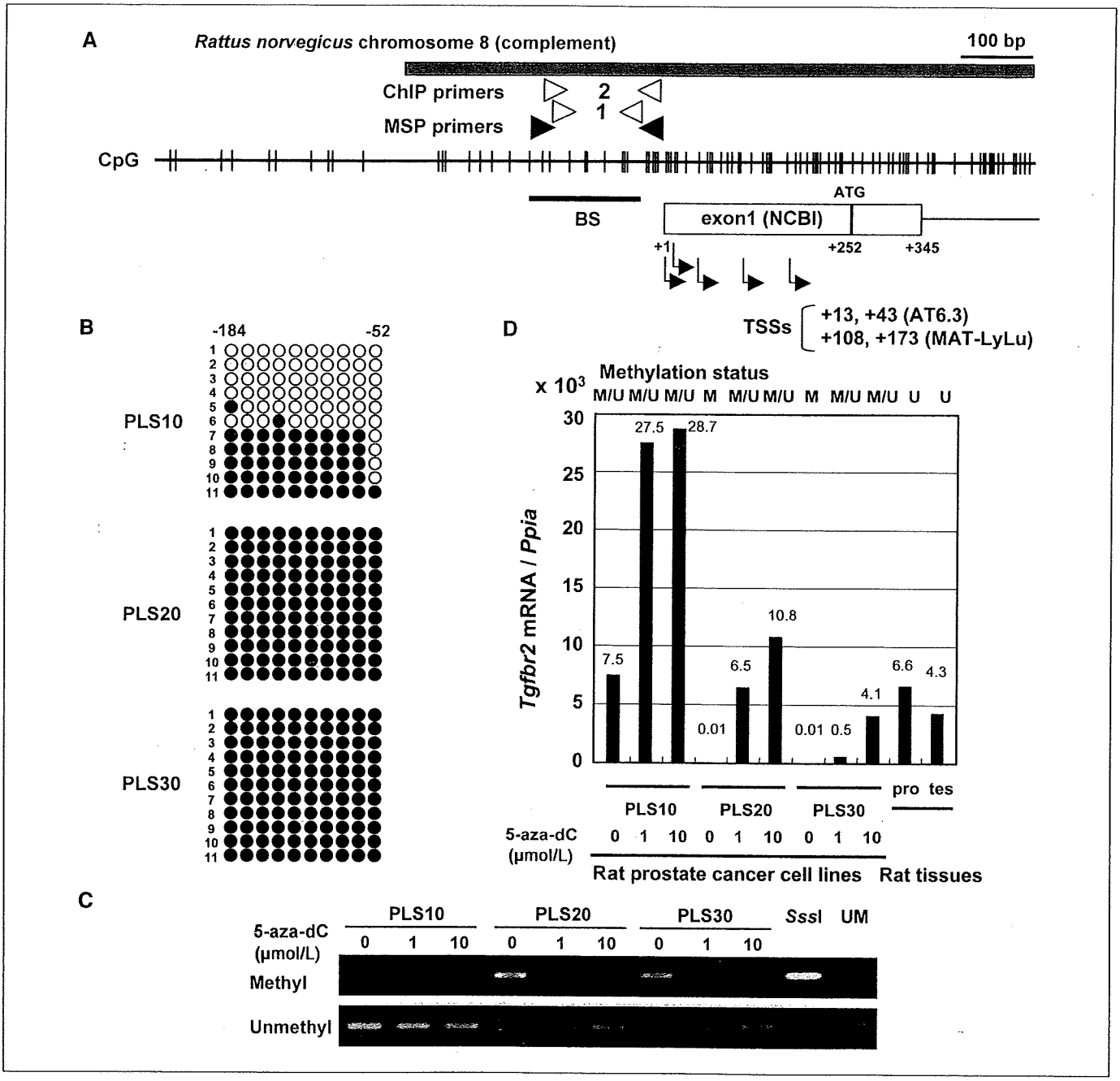

Figure 1. Methylation-silencing of *Tgfbr2* in rat prostate cancer cell lines induced by DMAB and testosterone. *A*, map of a promoter CGI, TSSs, and exon 1 of rat *Tgfbr2*. The TSSs were identified by 5′ RACE of AT6.3 and MAT-LyLu cell lines. *+1*, *Tgfbr2* TSS in the National Center for Biotechnology Information database (NC_005107.2, 120680453). *Vertical lines*, individual CpG sites; *gray box*, CGI region; *open boxes*, noncoding and coding exons; *arrows*, TSSs; *thick line*, the area analyzed by bisulfite sequencing; *arrowheads*, positions of MSP and ChIP primers. *B*, results of bisulfite sequencing in rat prostate cancer cell lines. The presence of dense methylation of the promoter CGI was confirmed for PLS20 and PLS30. *C*, *Tgfbr2* methylation status in rat prostate cancer cell lines analyzed by MSP. Demethylation was induced by 5-aza-dC in PLS20 and PLS30. *SssI*, genomic DNA methylated with *Sss*I methylase; *UM*, unmethylated control. *D*, quantitative mRNA expression analysis of rat *Tgfbr2*. *Tgfbr2* was expressed in the normal prostate (*pro*), testes (*tes*), and PLS10 that had unmethylated DNA molecules.